UNIVERSITÀ POLITECNICA DELLE MARCHE

FACOLTÀ DI INGEGNERIA

Corso di Laurea Magistrale in Biomedical Engineering

Involvement level assessment on acoustic jury tests based on EEG response

Relatore:

Prof.ssa Milena Martarelli

Tesi di Laurea di:

Sabrina Calderisi

A.A. 2022/2023

INDEX

CHAPTER 1 - INTRODUCTION 5

CHAPTER 2 - THE NERVOUS SYSTEM 6

2.1 Central nervous system and brain anatomy 6

2.2 Brain cells 13

2.2.1 Neurons 13

2.2.2 Glial cells 22

CHAPTER 3 - EEG INSTUMENTATION DEVICE 24

3.1 EEG instrumentation 24

3.2 EEG signals analysis 30

CHAPTER 4 - LATEST RESEARCH ON EEG 32

CHAPTER 5 - ACQUISITION PROCEDURE 38

5.1 Experimental setup 38

5.2 Muse Monitor sensors and recording device 40

5.3 EEGLAB 42

CHAPTER 6 - DATA PROCESSING 45

6.1 Muse Monitor autocleaning 45

6.2 Autoreject algorithms 50

6.3 Features calculation 53

6.3.1 Alpha wave 53

6.3.2 Alpha-Beta Ratio 56

6.3.3 Theta-Beta Ratio 59

6.4 Coherence analysis 62

CHAPTER 7 – CONCLUSIONS 66

BIBLIOGRAPHY 68

CHAPTER 1 – Introduction

Electroencephalography (EEG), a state-of-the-art technological innovation, possesses a potential that remains largely untapped. Its applications are not confined to the diagnosis of brain lesions, epilepsy, or other neurological disorders. Rather, it is emerging as a promising medical tool for the exploration, modelling, and elucidation of the intricate processes and mechanisms underpinning human brain function.

In the context of this research, an EEG Muse Monitor device was deployed to record neural signals while subjects were stimulated via acoustic stimuli during a jury test. These signals were subsequently processed using sophisticated software tools, namely EEGLAB and Matlab. One of the primary challenges encountered during this process pertained to the interpretation of EEG frequency bands most sensitive to the acoustic perception. Our current understanding of these frequency bands, while comprehensive in relation to sleep cycles and general brain activity, is limited when it comes to their response to motor activity, attention span, emotional states, the influence of various substances and specifically the perception of acoustic stimuli.

Following an exhaustive review of a wide array of scientific publications, it was hypothesized that the theta-beta ratio and the alpha-beta ratio are two critical parameters in qualifying a sound input and its subsequent impact on our mood and so, for future studies, sensory sensitivity in neurodevelopmental disorders. These ratios serve as valuable indicators, shedding light on the complex interplay between auditory stimuli and emotional responses. This finding underscores the potential of EEG technology in advancing our understanding of the human brain and opens up new avenues for future research.

CHAPTER 2 – The nervous system

The human brain is an astounding organ with an approximate weight of 1.5 kg [2.1] and is comprised of billions of cells. It is responsible for our capacity to perceive the world, think critically, and communicate effectively. As the human brain is commonly hailed as the most intricate organ within the body, its complexity continues to baffle researchers, leaving us with a profound lack of understanding regarding its functioning. For this reason, computational modelling and theoretical analysis have consistently proven essential in characterizing and comprehending the functions of nervous systems, as well as determining the interconnections between variables, timing, and causation involved in the process. [2.2]

An expression of this is neural coding, which is assuming a pivotal role in the study of cognitive functions. It is a field within neuroscience that focuses on understanding the hypothetical correlation between stimuli and neuronal responses, as well as the relationship among the electrical activities of the neurons within a group.

Building upon the theory that all information, sensory and otherwise, is represented in the brain through networks of neurons, it is believed that they can encode both digital and analog information. Statistical methods, probability theory, and stochastic point processes have been extensively employed to describe and analyse neuronal firing patterns. Thanks to advancements in large-scale neural recording and decoding technologies, researchers have commenced deciphering the neural code gaining initial insights into its real-time functioning during the formation and retrieval of memories in the hippocampus, a brain region crucial for memory consolidation [2.1] [2.3].

2.1 Central nervous system and brain anatomy

The central nervous system is composed by the union of the brain and the spinal cord. In its entirety, it consists of three fundamental parts, namely the *cerebrum*, the *brainstem*, and the *cerebellum*, as sketched in Figure 2.1. Functionally, the brain plays a critical role in governing and coordinating a wide range of bodily functions. It accomplishes this by collecting, organising, and integrating data from multiple sensory receptors. Furthermore, the intricate structures of the brain facilitate the recognition process, allowing us to make

rational decisions and effectively communicate instructions to other physiological components. [2.2]

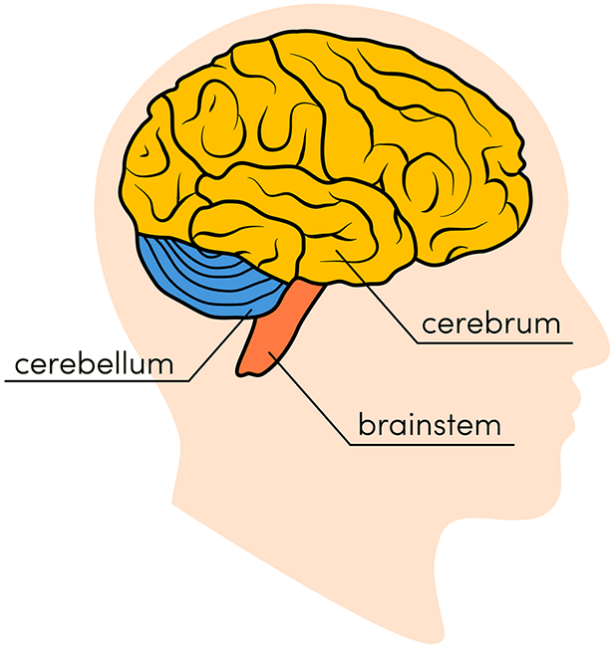

Figure 2.1 Main Parts of the Brain and Their Functions, Johns Hopkins Medicine website (https://www.hopkinsmedicine.org/health/conditions-and-diseases/anatomy-of-the-brain)

The cerebrum, the largest component of the human brain, receives and processes conscious sensations, generates thought, and regulates conscious behaviour. It is the brain's uppermost and largest part, divided into left and right hemispheres that are connected and communicate via the *corpus callosum,* allowing them to share information and work together. As a result, this bridge between the hemispheres is critical for integrating and coordinating various cognitive, sensory, and motor functions on both sides of the brain.[2.2] The decussation, word used to describe a crossing of nerve fibers, is the point where the nerves cross from one side of the brain to the other one, and it's why the left hemisphere controls the right arm movements, for example. It is the down-terminal part of hindbrain. [2.8]

Each hemisphere is composed by an inner core of white matter and an outer layer known as the cerebral cortex, composed of grey matter. The cerebral cortex further comprises the neocortex, forming the outermost layer, and the inner allocortex. Within the neocortex, there are six distinct neuronal layers, whereas the allocortex is formed by one main layer of

projection neurons sandwiched between layers that are rich in axons, dendrites and local circuit neurons.

Conventionally, each cerebral hemisphere is divided into five lobes, four of which have the same name as the bone over them: the frontal lobe, the parietal lobe, the occipital lobe, and the temporal lobe, see Figure 2.2. A fifth lobe, the insula or Island of Reil, lies deep within the lateral sulcus. [2.2]

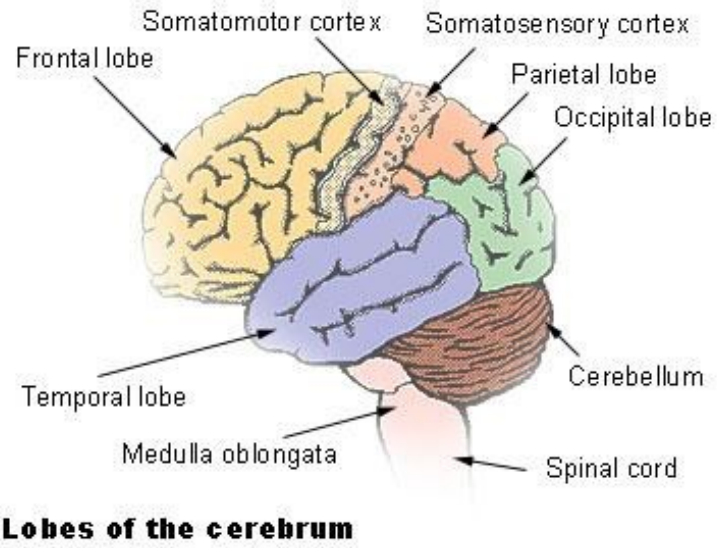

Figure 2.2 illustration of the different cerebrum lobes, U.S. National Cancer Institute's Surveillance, Epidemiology and End Results (SEER) Program website (https://training.seer.cancer.gov/index.html)

- The frontal lobe is responsible for executive functions, including self-control, planning, problem solving, and abstract thinking.
- The temporal lobe is responsible for sensory processing. Therefore, it also plays a role in memory formation and language comprehension.
- The parietal lobe is responsible for sensory integration, such as touch, temperature, and pain. It additionally assumes a significant function in the comprehension of spatial orientation and the perception of our surroundings.
- The occipital lobe bears the responsibility for the processing of visual stimuli. It is the recipient and processor of visual information originating from the ocular organs.

Within each lobe, specific regions of the cortex are associated with sensory, motor, and association functions. Furthermore, while the left and right hemispheres share many similarities in structure and operation, certain functions are lateralized, for example,

language is primarily located in the left hemisphere and visual-spatial ability in the right hemisphere. The connection between the hemispheres is facilitated by commissural nerve tracts, with the corpus callosum, serving as the largest tract. [2.2]

The cerebrum is interconnected with the spinal cord through the brainstem, as outlined in Figure 2.3. The latter is a critical part of the central nervous system and is composed of three distinct parts: the midbrain, pons, and medulla oblongata. The midbrain is the most superior part of the brainstem and is responsible for several functions, including vision, hearing, motor control, sleep and wakefulness, arousal, and temperature regulation. The pons is located in the middle of the brainstem and is responsible for relaying signals between different parts of the brain, as well as regulating breathing and sleep. The medulla oblongata is the most inferior part of the brainstem and is responsible for several autonomic functions, such as regulating heart rate, blood pressure, and breathing. [2.2]

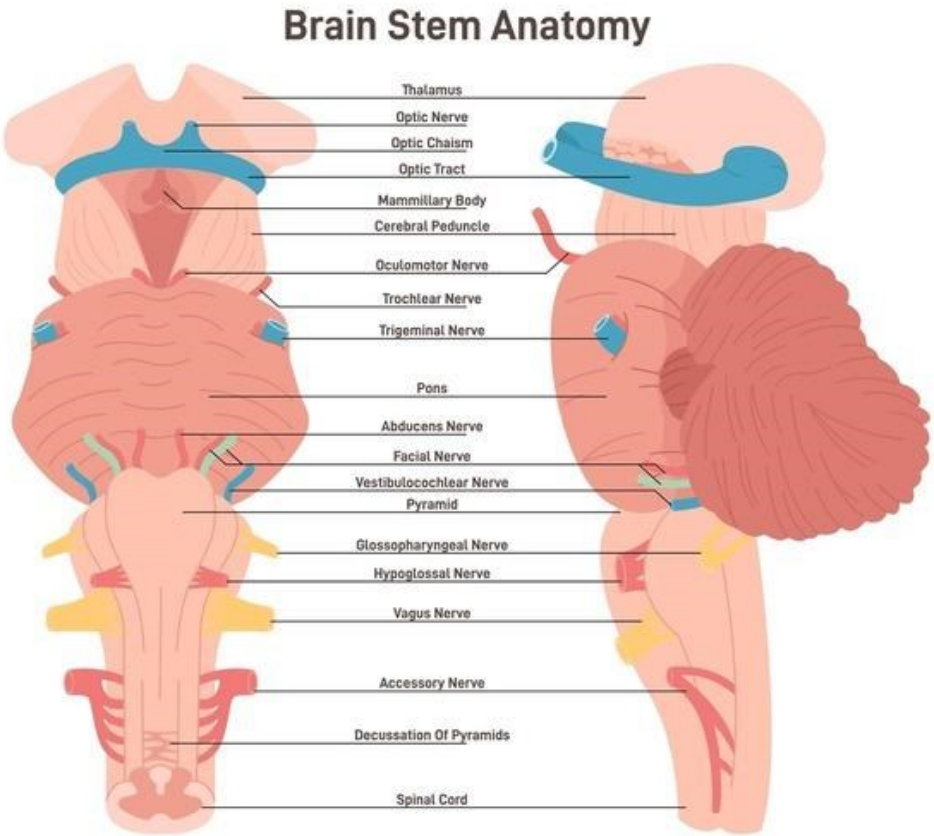

Figure 2.3 brain stem anatomy, Shutterstock website for scientific (STEM) illustrations

Together with the brain, our cranium contains the ventricular system. It is a network of interconnected cavities within the brain that are filled with cerebrospinal fluid (CSF), which is produced by the choroid plexus. The ventricular system is comprised of a quartet of ventricles: a pair of lateral ventricles, in conjunction with the third and fourth ones. The first two are the largest and are located in the cerebral hemispheres. The third ventricle is located in the diencephalon, while the fourth is located between the brainstem and the cerebellum. The ventricular system plays a crucial role in the production, circulation, and absorption of CSF, which provides mechanical and immunological protection to the brain and spinal cord. [2.2]

Beneath the cerebral cortex, several essential structures can be found. The thalamus is a large, egg-shaped structure that is located in the centre of the brain. It acts as a relay station for sensory information, processing and transmitting signals from the body to the cerebral cortex. The epithalamus is a small region of the brain that contains the pineal gland, which secretes the hormone melatonin and is involved in the regulation of circadian rhythms. The hypothalamus is a small but complex region of the brain that is involved in the regulation of many vital functions, including hunger, thirst, body temperature, and sleep. The pituitary gland, a structure of diminutive size akin to a pea, is situated at the basal region of the brain. It is frequently designated as the "master gland" due to its role in the synthesis of hormones that govern the functionality of other endocrine glands within the organism. The subthalamus, a compact region within the brain, participates in the orchestration of movement. [2.2]

In figure 2.4 it is schematized the cortical neuronal structure: cortical columns differ in terms of the number of layers, each having its own set of cell types and communication routes. The granular cortex consists of six different layers, the fourth of which contains granule cells that amplify and disseminate thalamocortical input. It also contains many spiny pyramidal neurons in its infragranular and supragranular layers. [2.10]
In contrast, the agranular cortex lacks a completely formed layer IV and has a hazy border between layers II and III. The top layers have fewer pyramidal neurons than layers V and VI. Despite the lack of a distinct layer IV, it continues to receive thalamic projections, but

the sensory information is amplified and redistributed less than in the granular cortex. The dysgranular cortex, found in transition zones between granular and agranular regions, has a small but defined layer IV and a distinctive layer II and III. [2.10]

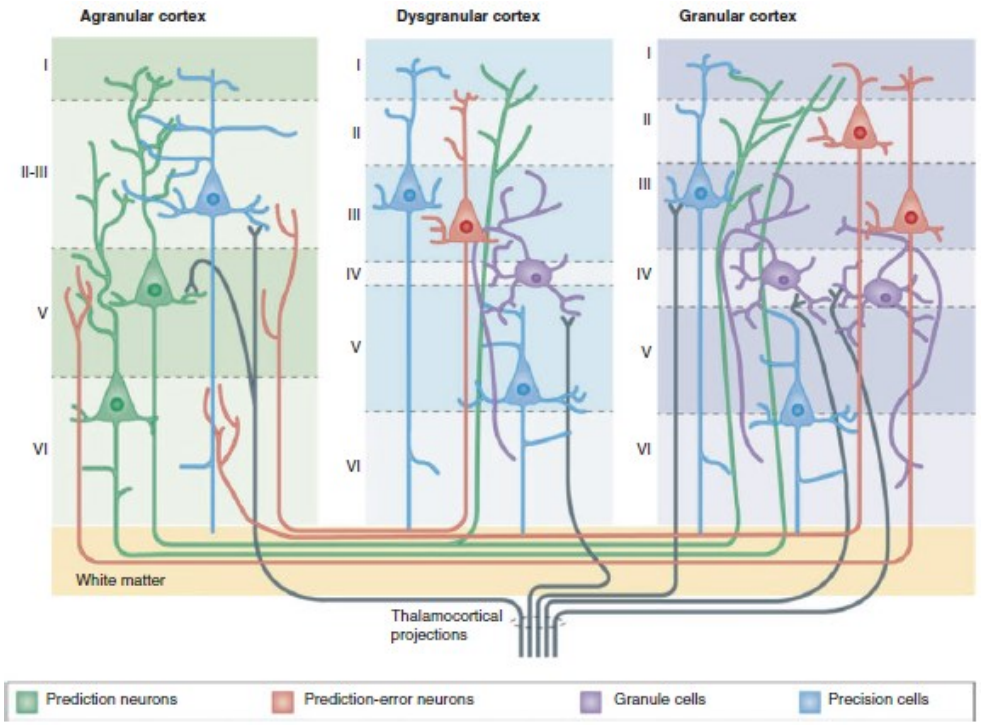

Figure 2.4 Organization and cellular architecture of cortical layers [2.10]

In Figure 2.5, instead, it is possible to visualise the *limbic system*. It is a group of interconnected structures posed at the centre of the skull, part of the brain, that are involved in the regulation of emotions, memory, and motivation. The amygdalae are almond-shaped structures that are situated in the temporal lobes of the brain. They are involved in the processing of emotions, particularly fear and anxiety. The hippocampi are a pair of curved structures that are located in the medial temporal lobes of the brain. They are involved in the formation and retrieval of memories. The claustrum is a thin sheet of grey matter that is located between the insula and the putamen. Its function is not well understood, but it has been suggested it plays a role in consciousness. The basal ganglia are a group of nuclei in the brain that are involved in the regulation of movement. The basal forebrain structures are a group of nuclei in the brain that are involved in the regulation of attention, learning, and memory. The circumventricular organs are specialised structures in the brain that lack a

blood-brain barrier and are involved in the regulation of fluid balance, body temperature, and hormone secretion. [2.4] [2.2]

A dysfunctional limbic system is associated with many clinical manifestations, such as epilepsy, limbic encephalitis, dementia, anxiety disorder and schizophrenia. [2.5]

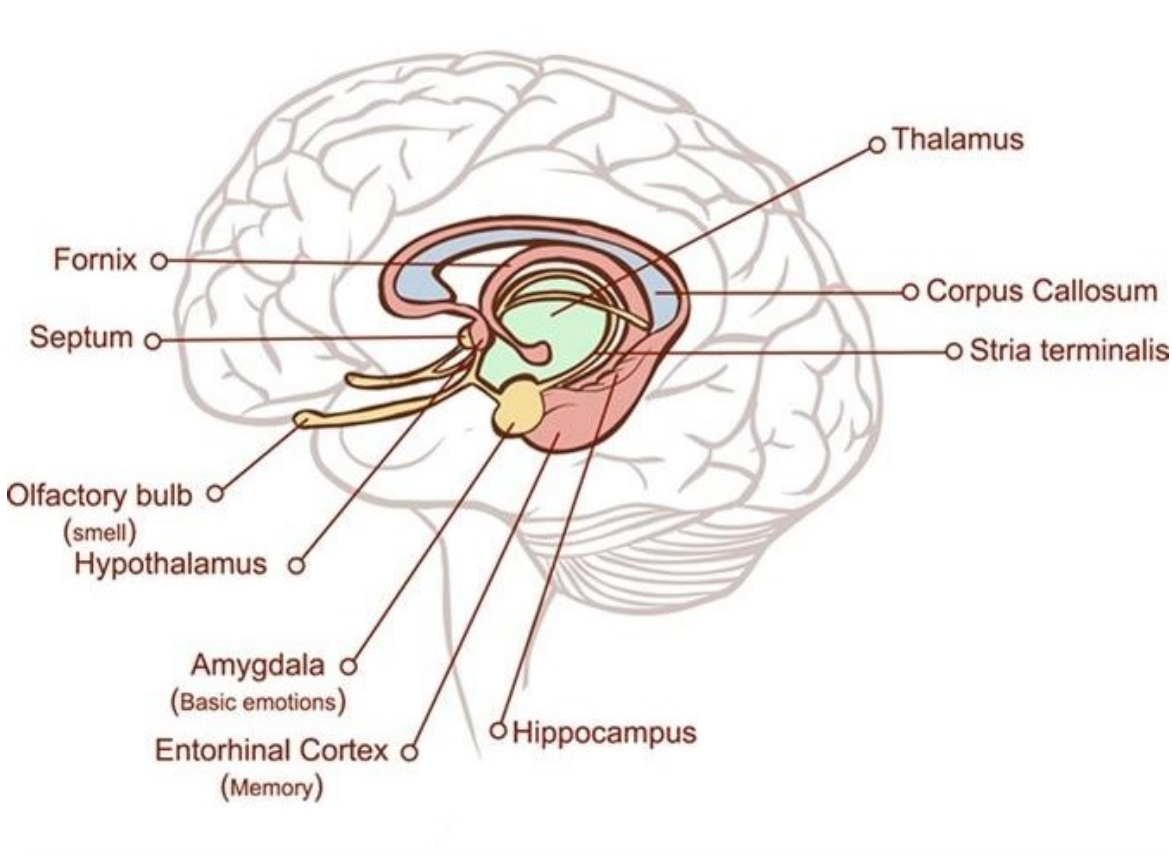

Figure 2.5 cross-section through the brain showing the limbic system and all related structures, Shutterstock website for scientific (STEM) illustrations.

The *spinal cord* is a long, tube-like band of tissue that runs through the centre of your spine, from your brainstem to your low back. It carries nerve signals for movement, sensation and reflexes. The spinal cord's main purpose is to carry nerve signals throughout your body. These nerve messages have three crucial functions. [2.2]

The operations and movements of the body are regulated by them. The brain dispatches signals to various parts of your body, dictating your actions. These signals also supervise

unconscious functions such as the rhythm of your breath, the beat of your heart, the respiration rate, and the workings of your bowel and bladder.

Signals from diverse parts of your body are relayed to your brain, aiding it in documenting and deciphering sensations like pain or pressure. [3.1]

Your spinal cord is also in charge of your reflexes. It controls certain reflexes (unconscious immediate movements) without the involvement of your brain. For instance, your spinal cord is responsible for your patellar reflex, which is the involuntary movement of your leg when someone taps a specific spot on your shin. The spinal cord is a delicate structure that contains nerve bundles and cells that carry messages from your brain to the rest of your body. Any damage to your spinal cord can affect your movement or function. [2.2]

2.2 Brain cells

The brain is composed of two main types of cells: neurons and glial cells. [2.8]

2.2.1 Neurons

Neurons are the proactive cells of the brain, that communicate between them and within the body via electrochemical signals using electrical stimuli and neurotransmitters: chemical messengers that carry messages from one neuron to another target cells affecting the whole nervous system and the body. [1.8] There are plenty of different neurotransmitters and their functions isn't always perfectly understood even nowadays. Some examples are:

- **GABA** (gamma-aminobutyric acid) that is the main inhibitor of synapses. Its molecule is shown in Figure 1.6. When in high quantity induces relaxation and focus while in a small amount causes anxiety. In fact, the main substances that induce a rise in GABA levels are anticonvulsant and anti-anxiety meds (usually benzodiazepine). [2.8]

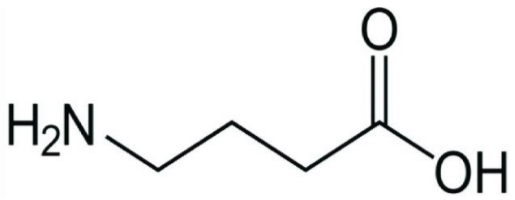

Figure 2.6 Gaba molecule (γ-Aminobutyric acid) [2.6]

– **Dopamine**, the main neurosignal involved in motivation, reward and pleasure. Its molecule is shown in Figure 2.7. Low dopamine levels are linked with certain health conditions like Parkinson's disease or depression, as well as disorders as ADHD. It could potentially heighten your propensity for risk-taking behaviour or the development of addictive tendencies. Can also cause problems with anger, low self-esteem, anxiety, forgetfulness, impulsiveness and lack of organizational skill. [2.8]

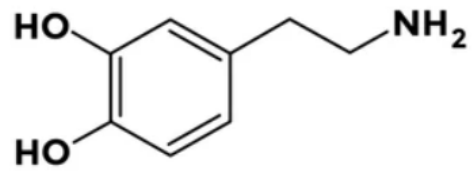

Figure 2.7 dopamine molecule, Shutterstock website for scientific (STEM) images.

– **Glutamate**, most abundant excitatory neurotransmitter in the human brain and central nervous system. Its molecule is shown in Figure 2.8. It plays a crucial role in various functions of the nervous system, including learning, memory, energy, sleep, and pain. Glutamate is naturally present in certain foods such as meats, seafood, milk, cheese, peas, tomatoes, and mushrooms. In high dosage is highly toxic for neurons. [2.8]

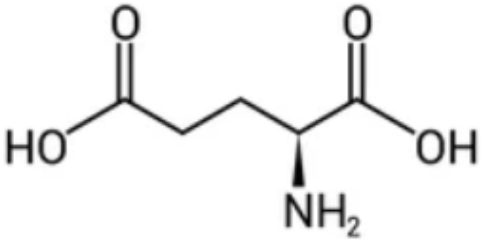

Figure 2.8 glutamic acid, *Shutterstock website for scientific (STEM) images*

– **Serotonin**, involved in pain sensation, digestion and sleep. Its molecule is shown in Figure 2.9. Is highly talked about as it is also involved in mood regulation and it is found in a low quantity in people who suffer from anxiety and depression and therefore is regulated by many antidepressants (for SSRIs) and anxiety

medications together with noradrenaline (as in the case of tricyclic antidepressants and SNRIs). [2.8]

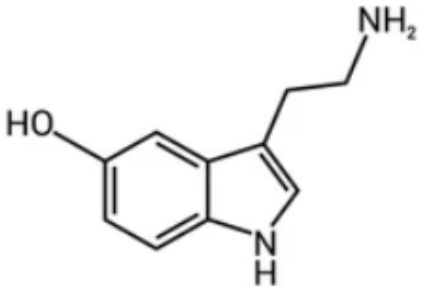

Figure 2.9 serotonin molecule, Shutterstock website for scientific (STEM) images

– **Noradrenaline (**or norepinephrine) is involved in alertness, attention, and the process known as "fight or flight". Its molecule is shown in Figure 2.10. A high noradrenaline level may cause anxiety while low concentrations are associated with low focus capacity and sleep disorders. [2.8]

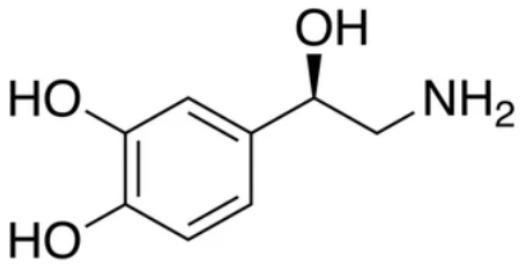

Figure 2.10 noradrenaline molecule, Shutterstock website for scientific (STEM) images

Neurons have a structure composed by a body (soma) one ore multiple dendrites and a longer connection called axon (see Figure 2.11). [2.8]

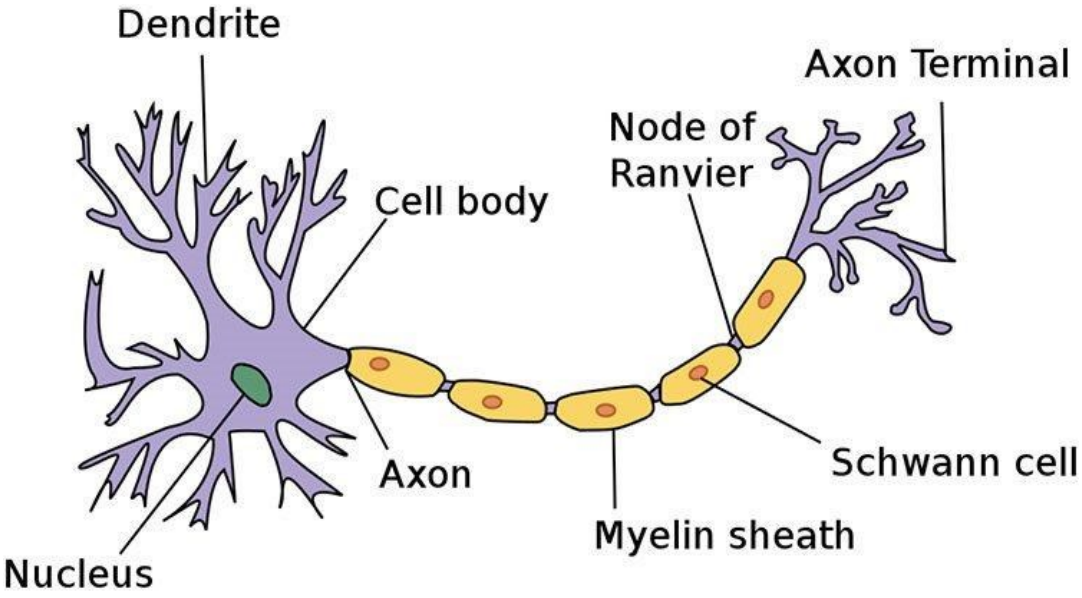

Figure 2.11 neuron structure, Shutterstock website for scientific (STEM) images

The soma contains the nucleus of the cell and keeps the cell alive, similarly as other eukaryotes cells. The dendrites are tree-like fibres that collect info and send it to the soma. The axon transmits the information using the transmembrane potential, a difference in electric potential between the interior and the exterior of a biological cell. [2.8]

The resting membrane potential (also called transmembrane potential or membrane voltage) is between -60 and -70 mV, and it's reached when electrical gradient (ions charge) is balanced by diffusion gradient (according to Fick's law), and it's maintained by the *Na+/K+ ATPase pump* (sodium-potassium pump, see Figure 2.12), which pumps 3 Na+ ions out of the cell and 2 K+ ions into the cell, creating a concentration gradient for both ions. [2.8]

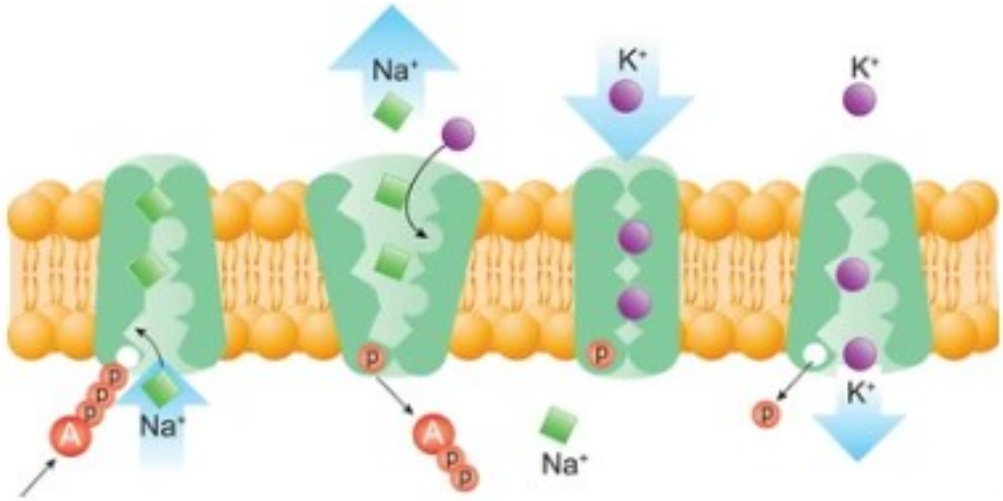

Figure 2.12 sodium-potassium pump, Shutterstock website for scientific (STEM) images

When a neuron is stimulated, the membrane potential changes, and if the change is large enough, an *action potential* is generated. An action potential represents a consistent alteration in the membrane potential, which is consequent to the sequential opening and closing of voltage-gated ion channels present on the cellular membrane. When the membrane potential reaches a certain threshold, voltage-gated Na+ channels open, allowing Na+ ions to flow into the cell, further depolarizing the membrane. This depolarization opens more voltage-gated Na+ channels, creating a positive feedback loop that rapidly depolarizes the membrane. When the membrane potential reaches a peak, voltage-gated K+ channels open, allowing K+ ions to flow out of the cell, repolarizing the membrane. The K+ channels remain open for a short time after the membrane potential returns to its resting state, causing an afterhyperpolarization. The action potential then propagates down the axon, triggering the release of neurotransmitters at the synapse, and is followed by a refractory period in which it's more difficult to reach newly the potential threshold needed. [2.8]

Action potential is an all-or-none event because it is either generated or not. In fact, if the stimulus is sufficient to push the membrane potential to pass the firing threshold for the neuron, an action potential is generated, and it is independent on the stimulus, otherwise it is not generated. From a chemical point of view, action potential is an

all-or-none event because it is generated only if Sodium channels open, and they close only when the membrane potential has overcome the zero value. [2.8]

The junction point of two different neurons is called *synapse*, so it's the point where the exchange of info takes place. There are electrical and chemical synapses. Electrical synapses have direct physical contact and enable the bidirectional passage of currents: the presynaptic action potential propagates to the postsynaptic cell, while the membrane resting potential of postsynaptic cell simultaneously propagates to the presynaptic cell. Chemical synapses involve neurotransmitters: the energy coming from action potential opens Calcium channels, so Ca++ ions come through synapses and release information. Some Ca++ ions are re-absorbed by presynaptic cell, but it's necessary that at least one ion reaches the postsynaptic to transmit the info, because when it attaches a receptor, the receptor opens Sodium channels. Postsynaptic potentials duration is between 10 and hundreds of milliseconds. Presynaptic potential duration is 2 ms and it's biphasic, while postsynaptic potential duration is more than 10 ms and it's monophasic (only depolarization). [2.8]

Electrical synapses have direct physical contact and enable the bidirectional passage of currents (see Figure 2.13): the presynaptic action potential propagates to the postsynaptic cell, while the membrane resting potential of postsynaptic cell simultaneously propagates to the presynaptic cell. Chemical synapses involve neurotransmitters: the energy coming from action potential opens Calcium channels, so Ca++ ions come through synapses and release information. Some Ca++ ions are re-absorbed by presynaptic cell, but it's necessary that at least one ion reaches the postsynaptic to transmit the info, because when it attaches a receptor, the receptor opens Sodium channels. Postsynaptic potentials duration is between 10 and hundreds of milliseconds. Presynaptic potential duration is 2 ms and it's biphasic, while postsynaptic potential duration is more than 10 ms and it's monophasic (only depolarization). [2.8]

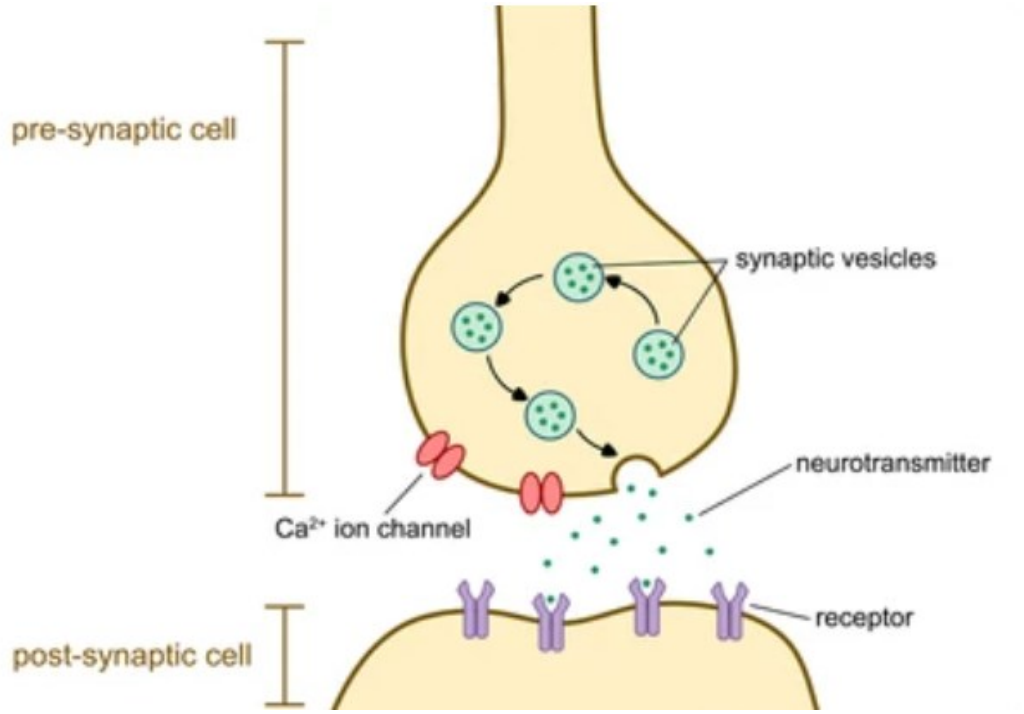

Figure 2.13 synapse, Shutterstock website for scientific (STEM) images

Summation of postsynaptic potential can be temporal or spatial. Temporal summation means that some close (in time) impulses are able to generate an action potential because the potential has no time to decrease. Spatial summation means that some impulses that are placed in different positions at the same time are able to generate an action potential. Impulses can be excitatory (EPSP, depolarizing) or inhibitory (IPSP, hyperpolarizing), and the number of useful impulses is the difference between these two types.

The *Hebbian theory* articulates that when the axon of a cell, denoted as 'A', is in sufficient proximity to stimulate cell 'B', or persistently contributes to its activation, a certain growth or metabolic modification transpires in one or both cells. This results in an enhancement of 'A's efficacy in its role as one of the cells triggering the firing of 'B'. This process is resumed by the phrase: fire together, wire together. So, two cells or systems of cells that are repeatedly active at the same time will tend to become associated, so that activity in one cell facilitates the activity in the other one. This phenomenon takes the name of *functional brain plasticity.* [2.8]

There are two levels of brain plasticity observation: cellular changes, due to learning, and large-scale changes, that means the cortical remapping in response to injury. So, the two kinds of brain plasticity are structural and functional. *Structural plasticity*, otherwise, is due both to new synaptic connections and to new nerve cells growing, so new neural networks are generated. Ramon y Cajal said that, given new cells cannot be produced, it can be supposed that cerebral exercise will lead to the development of new dendritic processes and axonal collaterals beyond that normal observed, forcing the establishment of new and more extensive intracortical connection. [2.8]

Neurons' structure can be divided into *unipolar*, *bipolar* or *multipolar*, as sketched as an example in Figure 2.14. [2.8] Physiologically, true unipolar neurons do not exist in the mature vertebrate nervous system. Therefore, all of the peripherical nervous system's basic sensory neurons are bipolar or pseudounipolar. Multipolar neurons contain multiple variably branching processes that extend in several directions; being the most frequent form of vertebrate neuron, they are the distinguishing feature of the human CNS. [2.11]

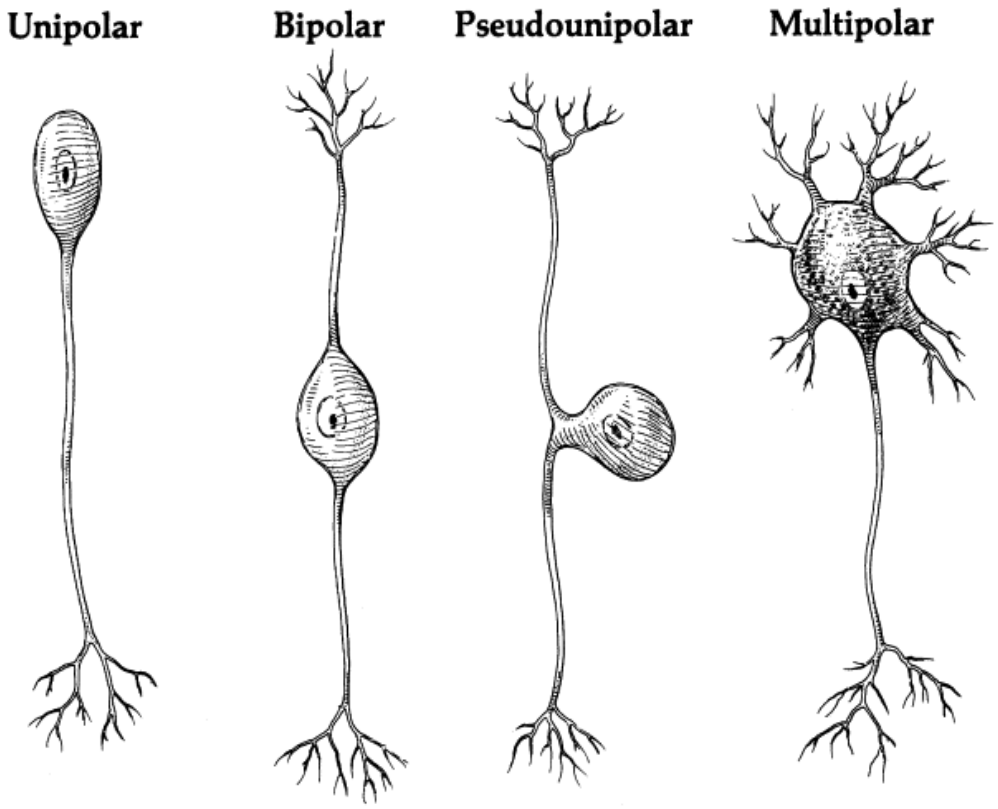

Figure 1.14 three general kinds of neurons are recognized: unipolar, bipolar, and multipolar. [2.11]

Unipolar neurons have a single process which divides into two branches: one to the CNS and the other one to the PNS; they generally are sensory neurons. Bipolar neurons have two processes: a dendrite and an axon; they generally are sensory neurons and can be found in sensory areas (ears, eyes, or nose). Multipolar neurons have an axon and many dendrites; the 99% of them are in the CNS and the mostly part of them are motor neurons. [2.8]

Functionally, instead, neurons can play three main roles: sensory, motor or can be interneurons. Sensory neurons collect info from internal (soft organs) or external environment, then they send info to CNS. Motor neurons transmit messages away from CNS to effector organs, employing peripheral neurons. Interneurons are in the CNS, they are generally multipolar and transmit info from one part of CNS to another one, so they process, store and receive info and make decisions in response. [2.8]

Neurons can also be described according the “direction” of the signal: they may be *afferent* (mainly sensory neurons) or *efferent* (mainly motor neurons). Afferent neurons transmit info from PNS to CNS, efferent from CNS to PNS. [2.8]

2.2.2 Glial cells

Glial cells compose the majority of the brain cell and provide physical and chemical support to neurons and their environment homeostasis. Their classification is shown in Figure 2.15. [2.8]

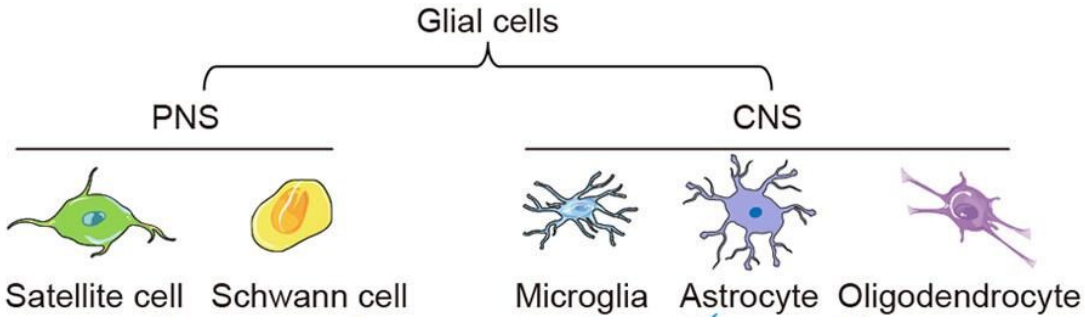

Figure 2.15 glial cells, Shutterstock website for scientific (STEM) images

There are 6 different types of glial cells, 4 of them are situated in the central nervous system and 2 in the peripherical nervous system. [2.8]

In the CNS there are astrocytes, oligodendrocytes, ependymal and microglia.

Astrocytes prevent the entering of undesirable substances in the brain via blood vessels, that they constrain by forming the Blood Brain Barrier. Furthermore, they help oligodendrocytes to perform better and are also important for the nutrition and structure of the NS.

Oligodendrocytes make myelin sheets around the axon (in CNS, while Schwann cells play the same role in PNS).

Ependymal cells line the cavities of the brain and spinal cord, and they regulate the exchange of several substances between the cerebrospinal fluid and the nervous tissue, so they are important for structure of the NS.

Microglia are phagocytes, so they engulf bacteria to protect the NS. [2.8]

In the PNS there are Schwann and satellites cells.

Satellites (PNS), support cell bodies (structural function). They are similar to the Schwann cells but are located around the cell bodies. Schwann cells make myelin sheets around the axon. [2.8]

CHAPTER 3 – EEG instrumentation devices

3.1 EEG instrumentation

Electroencephalography (EEG) is a common non-invasive neuroimaging method designed to measures the extracellular current flow generated by the spatio-temporal sum of post-synaptic potentials using electrodes, typically made of a conductive material such as silver chloride, positioned on the scalp of the patient arranged in a specific pattern on the cap, or net, to cover different regions of the brain. These postsynaptic action potentials have a duration that varies from tens of thousands of milliseconds, higher than that of the action potential and a maximum amplitude of 20mV, which tends to attenuate during propagation. The cerebral cortex, being the part of the brain closest to the scalp, is the one that contributes most to the development of potentials which are then measured with surface electrodes. The perceived signal is in fact the sum of the variations in the membrane potential of entire populations of neurons of the cortex. The neurons contained in the cortex are called cortical neurons and are distribute in 6 layers along the depth of the cortex, usually identified by I (the most near the cortex) to VI. The neurons contained here can be divided into pyramidal and non-pyramidal pyramidal depending on their shape. By observing this electrical activity, scientists can gain a better understanding of how the brain functions and how various cognitive processes occur. [3.3]

Measuring the electrical activity of neurons in the visual cortex, for example, can aid researchers in understanding how the brain processes sensory information or it can provide insights into how the brain regulates movement. Identifying abnormal patterns of electrical activity in the brain can also provide help in understanding the underlying mechanisms of neurological disorders such as epilepsy, Parkinson's disease, and Alzheimer's disease, helping develop new treatments and therapies for these conditions by identifying abnormal patterns of electrical activity in the brain. See Figure 3.1, 3.2 and 3.3 to have a hint about the typical signal anomalies related to neurological disease. [3.2] [3.3]

Observing the electrical activity of neurons can also assist researchers in the development of brain-computer interfaces (BCIs), which are assistive technology devices that allow people

to control computers or other electronics via brain activity. [3.1] For example the control of robotic prosthetic limbs, communication assistive devices, and cognitive enhancement devices for some neurological condition patients or neurodevelopmental disorders compensation training. [3.3]

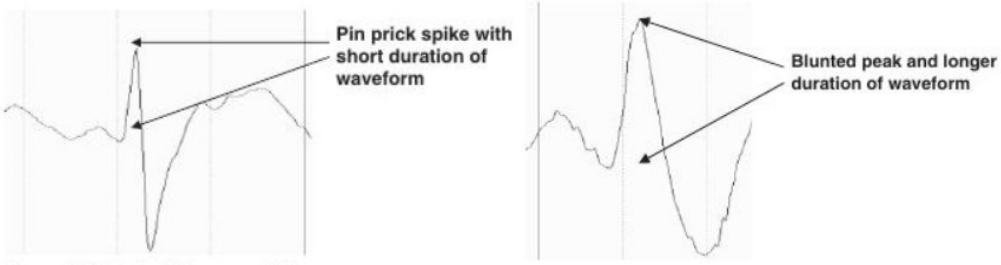

Figure 3.1 – spike 200ms per division.[3.2] || *Figure 3.2 – sharp wave followed by a slow wave. 200ms oer division.[3.2]*
Examples of EEG abnormalities that are present in patients with brain lesions and epilepsy

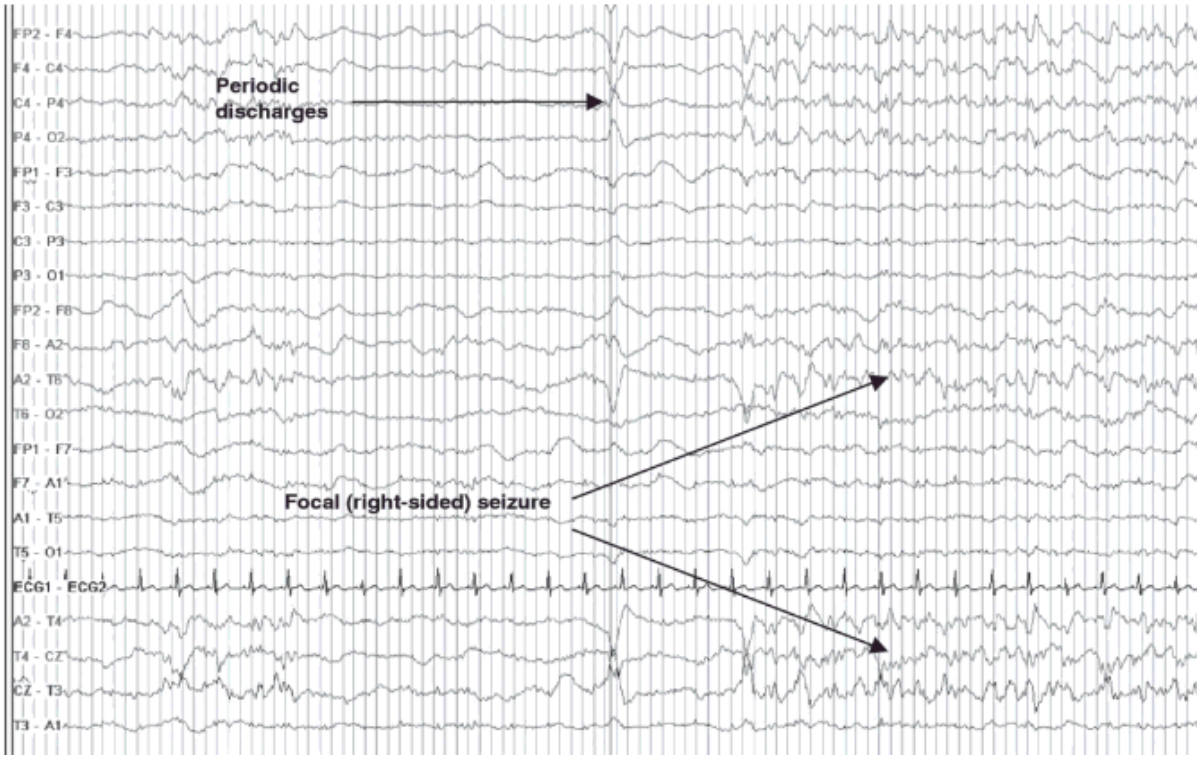

Figure 2.3 herpes simplex encephalitis showing periodic discharges; a right-sided focal seizure. 100 ms between vertical lines [2.2]

Several elements are included in the EEG apparatus. As previously stated, electrodes are an essential component. Each electrode is applied to the scalp with conductive gel or paste to

improve the contact between the electrode and the skin, and to reduce electrical impedance. [3.1] [3.3] The electrodes are usually arranged on the scalp according to the 10/20 standard, adopted by the American EEG Society (Barlow et al, 1974).

The standard initially proposed included 21 electrodes, which are arranged at 10% and 20% of the arcs coronal, sagittal, circumferential, between 4 points: nasion, inion (2 anatomical landmarks), A1, A2 (as it is visible in figure 3.4 and 3.5). The electrodes are identified by an alphanumeric code depending on their position on the head: Fp for fronto-polar, F for frontal, C for central, P for parietal, T for temporal, and O for occipital. Odd numbers refer to electrodes on the left side and vice versa, while z denotes electrodes along the line median. In order to make accurate EEG readings, the reference electrode is crucial as well. It offers a starting point (or so-called point of comparison) for measuring the electrical activity of the brain. Among the electrodes, the ground electrode is placed in a neutral zone of the head, usually the forehead. [3.3]

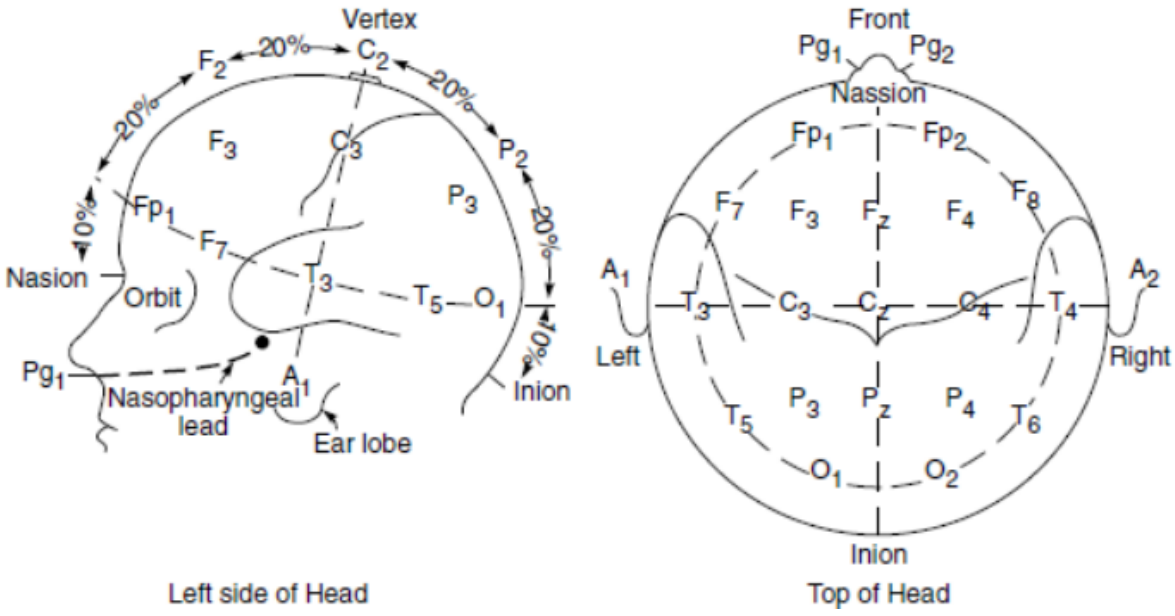

Figure 3.4 International 10/20-system. [3.3]

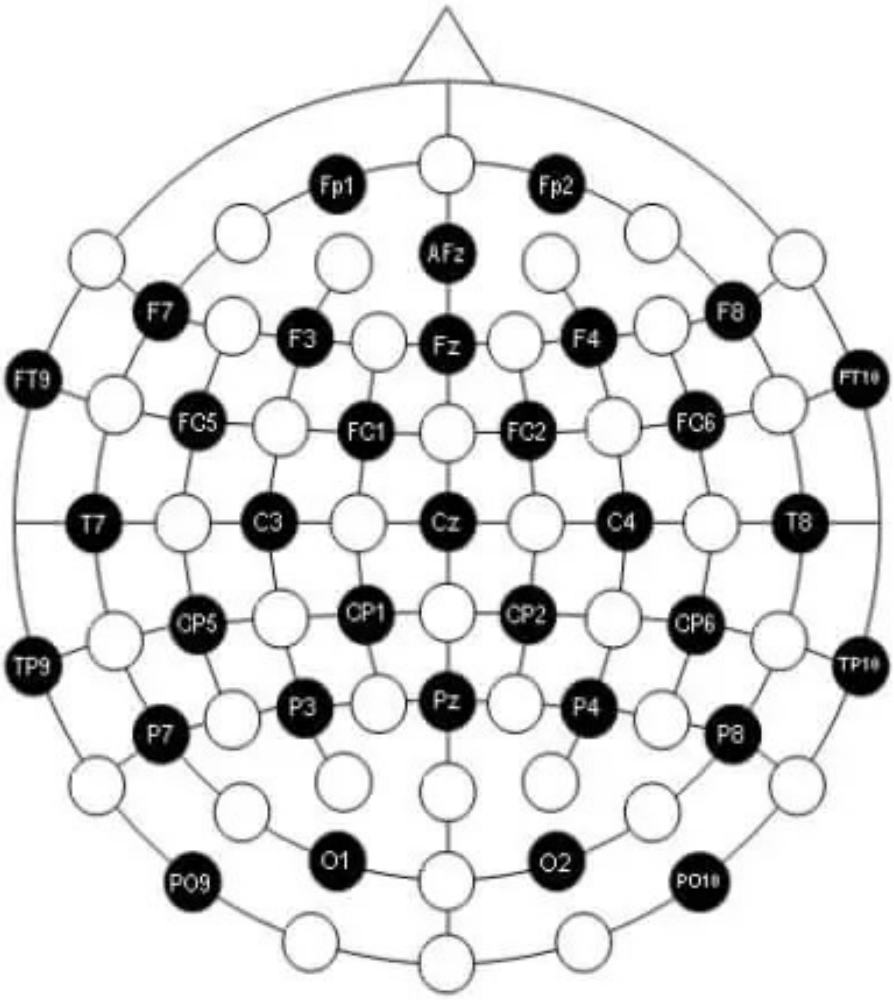

Figure 3.5 International 10/20-system. [3.3]

Additional electrode placement techniques can employ high-density EEG systems, availing a larger number of electrodes, that can expect up to 128 acquisition points, and providing more precise spatial resolution of brain activity. These systems often are used with customized electrode caps with predefined electrode positions. [3.1] [3.3]

Electrodes can be differentiated by the different materials involved [3.4]:

- Soft gel-based electrodes connect to the scalp by placing a conductive gel in each electrode's designated pocket. After the experiment, clean the headset by removing the gel and thoroughly cleaning the electrodes. Alcohol is commonly used for this cleaning process because of its evaporative properties.

- Some EEG headsets use conductive gel to create a low-impedance electrical connection between the skin and the sensor electrode. In these headsets, electrodes are connected by applying saline solution to each one.
- Dry: These devices do not require gel or saline to establish electrode-to-scalp contact, making it easier to record EEG data without the assistance of a trained technician. Furthermore, dry devices require significantly less setup time than wet headsets.
- Others: Some EEG sensor connection types do not fit cleanly into either of these two categories. Conductive substances in a solid gel state, exemplified by those fabricated by Enobio, have been efficaciously utilized in electroencephalogram apparatuses.

The typical measurement chain of an EEG system is given in Figure 3.6.

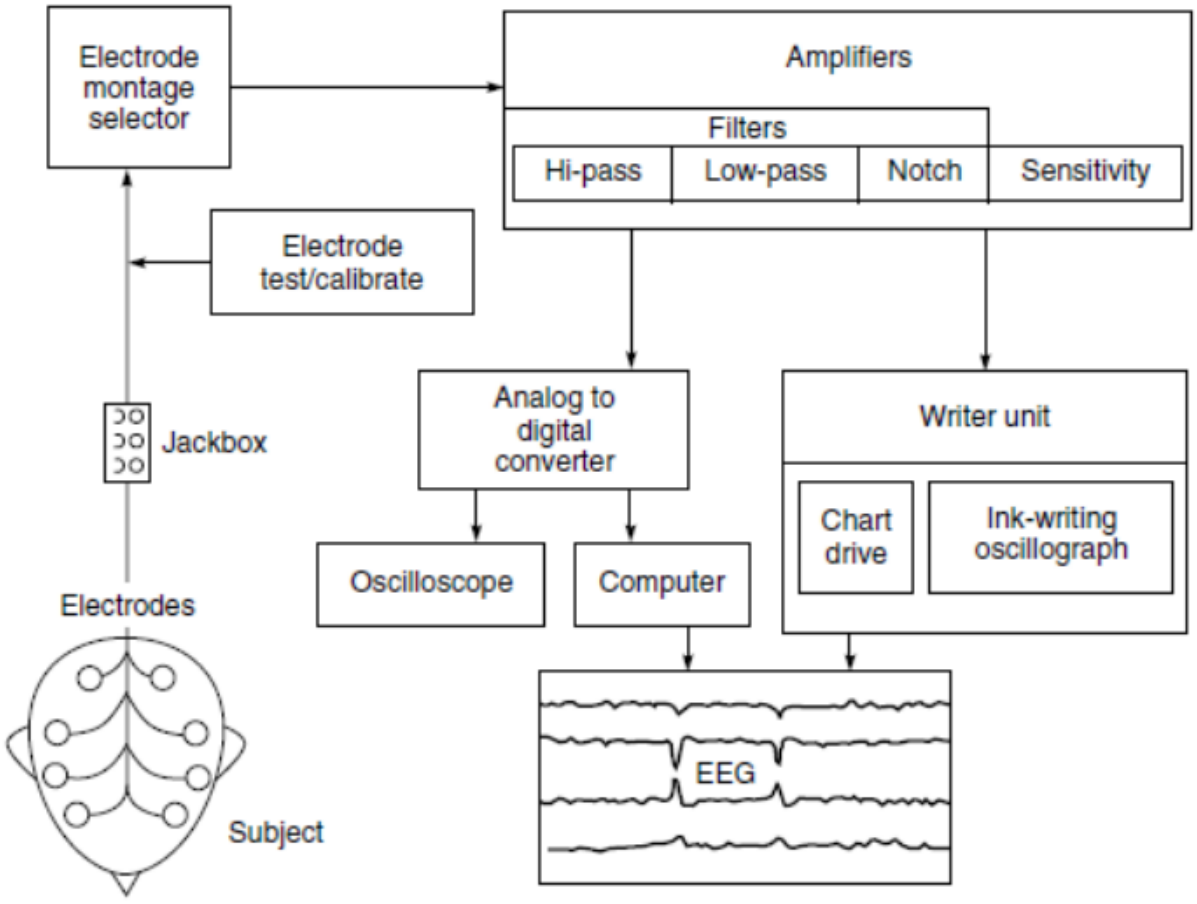

Figure 3.6 block diagram of an EEG instrumentation device, with both analogue and digital components. [3.4]

The EEG signals are transmitted from the electrodes to the Jackbox, labelled according to the 10-20 standard, and then get to the electrode selector where you can set bipolar or unipolar leads; in the case of an analogue machine, the selector is a large panel containing switches that allow the user to choose the various pairs of electrodes to subtract. In the modern digital electroencephalographs, a unipolar assembly is often preferred which allows to choose any different type of editing after digitization. [3.4]

The electrodes are connected to the jackbox by the input cable. The EEG patient cable is designed to be flexible and comfortable for the patient, allowing them to move and be comfortable during the diagnostic or monitoring procedure. It is often made with lightweight materials and may have a length suitable for the specific needs of the healthcare facility. The cable length choice is important for the signal quality too: the length of the EEG cable should be sufficient to connect the EEG electrodes on the participant's head to the EEG amplifier, but longer cables may increase the chance of signal degradation and interference. [3.3] [3.4]
It's also important to ensure that the EEG system, including the cables, is properly shielded to minimize electrical noise. It is important to periodically inspect cables for damage and replace or repair them when necessary to maintain optimal recording quality as it's well known in the field that the patient cable, due to its frequent handling during EEG setup and removal, can be prone to wear and tear. [3.3]
In addition to transmitting the electrical signals, the patient cable may also include additional features such as impedance testing. This allows the healthcare professional to ensure that the electrodes are properly attached, and the signal quality is optimal.

Another essential element of EEG gear is the amplifier. The raw EEG signal has amplitudes of the order of μV and contains frequency components above 300 Hz. Since the incoming electrical impulses have low amplitude, cleaning them from interference or noise is crucial to allow a clean reading and analysis. A good amplifier should have high input impedance, low noise, and wide bandwidth to accurately detect and amplify the brain signals. The ability to digitise signals and store them for subsequent examination is a characteristic of modern amplifiers. [3.3]

The amplified EEG signals are pre-processed by signal conditioning circuits to remove noise, filter undesired frequencies, and increase the signal amplitude from the desired frequency bands. EEG machines can be stand alone or a computer-based system equipped with data acquisition interfaces. [3.1]

Other characteristics of a device include:
-sampling rate, that determines the temporal resolution of the recorded brain signals and should be high enough to capture the desired frequency content of the brain activity.
The typical sampling rate for electroencephalography (EEG) is based on the Nyquist-Shannon theorem. The minimum sampling rate should be at least 256 samples per second; however, a sampling rate of 512 Hertz (Hz) is preferred to prevent "aliasing", which is high frequencies falsely appearing as lower frequencies on screens of high resolution computers. Generally, a sampling rate between 250 Hz and 1000 Hz can be sufficient. [3.7]
-electrode impedance monitoring, and impedance checkers, that measure the electrical resistance between the electrode and the scalp, providing real-time feedback on the electrode-skin contact. [3.1]

Furthermore, open-source software programmes such as MNE-Python and EEGLAB are frequently used to process EEG data. EEG signal analysis can be performed with a wide range of methods, including spectral power analysis, which evaluates the power distribution of different frequencies in the EEG signal, and coherence analysis, which investigates signal synchronisation between different regions of the brain. [3.1]

3.2 EEG signals analysis

As a non-stationary and asymmetric physiological signal, EEG has a low signal-to-noise ratio (SNR), which brings great challenges to the extraction and selection of robust features of emotional EEG. Traditional EEG features mainly include time domain features, frequency domain features and time–frequency domain features. [3.5]

Compared with the other two kinds of EEG features, frequency domain features have been proved to be more effective. The common method of frequency domain feature extraction is to decompose EEG signals into:

- Delta band (0,5-4Hz) – present mostly the first year of life, in adults usually associated with deep sleep. It can also detect anomalies even in the absence of documented structural lesions. [3.2][2.8]
- Theta band (4–7 Hz) – usually irregular in the awake state and is of greatest amplitude in the posterior temporal region. [3.2] It's considered normal in young children and can be observed during drowsiness, light sleep stages, arousal [3.8] [3.9] in older individuals, and even during meditation. [3.2] [2.8]
- Alpha band (8–13 Hz) – the dominant rhythm present during wakefulness, mostly over the posterior region of the brain: usually the maximum amplitudes (belox 50 μV) are visible over the occipital area. Best seen with eyes closed and during physical relaxation and relative mental inactivity. [3.2][2.8]
- Beta band (14– 30 Hz) – mostly associated with normal waking consciousness. Low-amplitude Beta waves with multiple and variable frequencies are often associated with active, busy or anxious thoughts and active concentration. Above the motor cortex, Beta waves are associated with muscle contractions that occur in isotonic movements and are suppressed before and during movement changes. [2.8]

Frequency domain features mainly include power spectral density (PSD) feature, differential entropy (DE) feature, differential asymmetry (DASM) feature and rational asymmetry (RASM) feature, among which DE feature has the best performance. [3.5]

Some studies like Zheng et al. [3.6] utilized deep neural networks to identify the most effective frequency bands for EEG-based emotional response recognition, revealing for example that Beta and Gamma bands are most effective for classification tasks, and suggest that EEG signals from different emotional states show significant spatial, frequency, and temporal variations.

CHAPTER 4 – Latest research on EEG

The significance of the magnitude of the power spectrum density, derived from the differential frequency bands, is not solely associated with the commonly recognized levels of wakefulness. Extensive research has been conducted to explore the utility of EEG in the examination and observation of movement disorders such as ataxia, tremor, and dystonia. These studies have focused on the synchronization of cerebellar activity both internally and in conjunction with the cerebral cortex [4.1].

Furthermore, EEG has been employed to evaluate the efficacy of pharmaceutical treatments [4.2] and to possibly diagnose disorders such as Alzheimer's disease [4.3]. It has also proven instrumental in the study of more intricate sleep disorders [4.4].

Of paramount interest to this project is the exploration of the correlation between EEG frequency waves and the recognition of complex human emotions. Specifically, we aim to investigate potential parameters that can be extracted from EEG data, thereby providing a robust framework for emotion recognition. This endeavour holds significant promise for advancing our understanding of the intricate interplay between neurophysiological signals and emotional states. Previous study indicates that increased brain activity correlates with emotional and cognitive functions. Frequencies were categorised based on their prominence in different mental states. High frequency bands (Beta and Gamma) provide greater discriminative information for emotion identification compared to lower ones. [4.15]

The investigation of annoyance, and more broadly, the evaluation of emotional responses following exposure to stimuli through EEG signal analysis, represents a burgeoning area of research. Numerous studies have delved into the relationship between *alpha waves* and annoyance, especially within the context of sensory irritants such as noise. Findings suggest that annoyance is correlated with a decrease in alpha wave power, indicative of increased attention and vigilance towards the irritating stimulus. The alpha-band has emerged as a prominent EEG indicator in this regard, demonstrating robust measurement, test reliability, and high reproducibility. Furthermore, it has been shown to be capable of detecting early stages of fatigue and annoyance, underscoring its potential utility in this field of study [4.5]. The enhancement of alpha waves has been the subject of extensive research, particularly in

relation to the treatment of cognitive disorders. This includes conditions such as Alzheimer's disease, where the modulation of alpha wave activity may hold therapeutic potential. This line of inquiry underscores the pivotal role of alpha waves in cognitive functioning and the broader implications for neurodegenerative disease management. [4.6].

Two key articles have explored the relationship between alpha waves and attention. These could prove valuable in studying sensory stimuli, as when they are perceived as enjoyable are thought to be more effective in capturing attention:

- Barry et al. [4.11] reviews the event-related potential (ERP) literature in relation to attention-deficit/hyperactivity disorder (ADHD). It explores various aspects of brain functioning in ADHD, ranging from early preparatory processes to a focus on the auditory and visual attention systems, and the frontal inhibition system1. The research to date has identified a substantial number of ERP correlates of ADHD. However, the article does not specifically mention beta waves.
- Klimesch et al. [4.12] discusses the role of alpha-band oscillations in the human brain. It suggests that alpha-band oscillations have two roles (inhibition and timing) that are closely linked to two fundamental functions of attention (suppression and selection), which enable controlled knowledge access and semantic orientation2. This paper does not specifically discuss beta waves.

Another key frequency bands discernible in EEG signals is the *theta band* [4.7]. Theta waves are typically associated with states of deep relaxation, meditation, and creativity. They are frequently observed during periods of drowsiness or tasks that necessitate focused attention. In the context of sensory stimuli, an increase in theta power may signify a state of relaxation or engagement with a novel sensory stimulus, a demanding cognitive task, or a situation requiring substantial cognitive resources in general [4.8] [4.9] [4.10].

Three primary articles have been consulted regarding alpha and theta wave analysis:

- Klimesch et al. (1999) [4.8] examines the relationship between EEG alpha and theta oscillations and cognitive and memory performance. The author discusses two types of EEG phenomena associated with good performance: an overall increase in alpha power and a decrease in theta power, and a specific event-related decrease in alpha

power and increase in theta power depending on the memory demands. The article highlights that a higher degree of alpha desynchronization is linked to better long-term memory performance, specifically semantic memory. Additionally, the author finds that theta synchronization is positively correlated with the ability to encode new information.

- Snipes et al. [4.9] examines the differences in theta oscillations during cognitive tasks and sleep deprivation. They found that both cognitive load and sleep deprivation led to increased theta power in the medial prefrontal cortical areas. However, sleep deprivation also resulted in additional increases in theta activity in mostly frontal areas. The specific sources of theta activity during sleep deprivation varied depending on the task being performed.
- Başar et al. [4.10] presents the argument that specific delta, theta, alpha, and gamma oscillatory systems are distributed selectively and serve as resonant communication networks involving numerous neurons. Consequently, these oscillatory processes likely have a crucial function in facilitating communication and coordination within the brain, particularly regarding memory and integrative functions. The paper discusses the role of alpha-band oscillations in the human brain. Alpha-band oscillations are the dominant oscillations in the human brain and recent research indicates that they have an inhibitory function. However, the paper also suggests that alpha-band oscillations play an active role in information processing.

  This study proposes that alpha-band oscillations have two roles: inhibition and timing. These roles are closely linked to two fundamental functions of attention: suppression and selection. These functions enable controlled knowledge access and semantic orientation, which is the ability to be consciously oriented in time, space, and context.

Conversely, *beta waves* are high-frequency oscillations ranging between 12 and 30 hertz. They are often linked to the ability to think clearly and active mental activity. When engaged in tasks that require focus, problem-solving, or sensory processing, beta activity tends to increase. An increase in Beta power in the context of sensory inputs might indicate heightened attention or cognitive processing [4.8] [4.11] [4.12]. Beta waves have been studied for their potential to differentiate emotions such as happiness, sadness, calmness, and anger [4.13]:

- In the conducted experiment of Mehmet Bilal Er et al. [4.13], 9 individuals participated in a quiet and dark environment. A selection of songs from various music genres were played to the participants. While listening to the music, the EEG signals of these subjects were recorded on a computer with an EEG recorder simultaneously. At the end of each song, the subject was asked about the emotion they experienced and labeled the recorded EEG signals accordingly. These labels were described as feelings of anger, sadness, happiness, or relaxation.

  The recorded and labelled EEG signals were initially passed through a bandpass filter to obtain individual spectrogram images in the alpha and beta frequency bands. No additional effort was made to extract the feature. After a data augmentation process was applied to the obtained spectrograms, a transfer learning process was applied using previously trained deep networks. AlexNet and VGG16 were used as deep networks.

  The best classification result was obtained with the Beta frequency band spectrograms and VGG16 at 73.28%. According to the results, it is asserted that pre-trained deep learning models could be used for the problem of recognizing human emotions. It was also determined that pre-trained deep architectures are a very effective method, even if the original training data is limited.

To gain a deeper understanding of the role of theta and beta waves in sensory processing, researchers often compute specific ratios. The theta-beta ratio, which compares the power of the theta and beta bands, is one such metric. A higher theta-beta ratio may indicate a relaxed mood or enhanced sensitivity to sensory inputs, while a lower ratio may suggest a more concentrated or engaged state [4.14].

Similarly, the alpha-beta ratio compares the strength of the alpha band to that of the beta band. Given that the alpha band is frequently associated with states of relaxation and ease, a higher alpha-beta ratio may indicate a relaxed state or reduced sensory processing. Conversely, a lower ratio may suggest more active cognitive engagement with sensory stimuli [4.14].

The parameters referenced represent merely a fraction of the potential variables considered throughout the duration of the studies [4.16]. Over time, a multitude of additional metrics have been developed, evaluated, and compared, as depicted in Figure 4.1

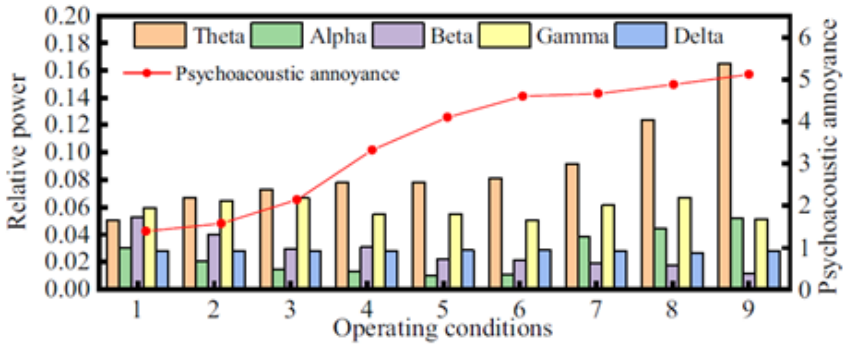

Fig. 14. the relative power of EEG sub-band under the psychoacoustics annoyance.

Table 7
The selection of EEG psychoacoustics annoyance index

Traditional index	Index	Formula	Description
	1	$\beta/(\theta+\alpha)$	Inverse index of detecting fatigue [68]
	2	α/β	A feature for determining whether people are attentive [69]
	3	β/α	Detecting fatigue [68]
	4	$(\alpha+\beta)/(\alpha+\theta)$	Inverse index of detecting drowsiness [69]
	5	β/θ	Inverse index of detecting drowsiness [69]
	6	θ/β	A marker for cognitive over-attention to the mild and high threat [70]
Index by Wang	7	β/δ	A marker for attention [71]
	8	$\theta/(\beta+\gamma)$	Proposed by Wang et al., similar to Index 1 [29]
	9	$\alpha/(\beta+\gamma)$	Proposed by Wang et al., similar to Index 2 [29]
	10	$(\beta+\gamma)/\alpha$	Proposed by Wang et al., similar to Index 1 [29]
Proposed annoyance index	11	$(\delta+\theta+\alpha)/(\beta+\gamma)$	Proposed by authors, similar to Index 1
	12	$(\theta+\alpha)/(\beta+\gamma)$	Proposed by authors, similar to Index 2
	13	$(\theta+\alpha)/\beta$	Proposed by authors, similar to Index 2

Figure 4.1 EEG annoyance indexes [4.16]

The analysis of frequency bands and their associated ratios in EEG data provides valuable insights into the brain's response to sensory inputs. This contributes to our understanding of the cognitive processes involved in sensory processing, relaxation, and concentration. By investigating the different parameters discussed, it is possible to gain a more comprehensive understanding of how the brain responds and adjusts to diverse sensory inputs in different cognitive states.

In summary, we can conclude that EEG features most fitting with annoyance are alfa, beta and theta waves and even more the alpha/beta and theta/beta ratios. The correlation of those features with pleasant and annoying sounds are reported in Table 1.

Table 5.1 Feature – annoyance correlation

Feature	Pleasant	Annoying
Alpha	↑	↓
Beta	↓	↑
Theta	↑	↓
Alpha/beta	↑↑	↓↓
Theta/beta	↑↑	↓↓

CHAPTER 5 – Acquisition procedure

5.1 Experimental setup

The experiment was performed on 44 subjects, in an isolated location. The subjects were asked to avoid food and water one hour before the procedure took place in order to avoid external influence on neural activity [5.1] [5.2].

The volume of the headphones was meticulously adjusted in accordance with each participant's personal tolerance level, ensuring a comfortable and consistent auditory experience across the board. Cameras were strategically positioned to enable continuous observation of the participants throughout the duration of the experiment. The participants were seated in a comfortable chair at a distance of about 70 cm from the screen, see Figure 4.1. They were instructed to sit still, relax their muscles and try to minimize eyes movements during the course of a trial. The headband was adjusted to the comfort of the participant.

Figure 5.1 example of experimental setup of a subject during the test

The volunteers were presented with a privacy information sheet to sign, along with another document elucidating the purpose and objectives of the study. This was followed by a comprehensive briefing session where each participant was instructed on the protocol of the test, thereby preparing them for the expected conduct during the experiment.

At this point, three different audio emissions have been alternated with pauses in which the subject's brain had time to return to neutrality, to avoid sensory overload and correctly separate different EEG signal adaptation to auditory stimuli without each other influence: the first audio was the sound of a car engine speeding up, which can be considered a neutral stimulus since can be perceived subjectively both pleasant and unpleasant. The second stimulus was a soothing and presumably appealing song played on the piano, while the third and last audio was a negative and irritating emotion triggering sound made by a crowd of people in a public area.

60s	60s	60s	60s	60s	60s
Silence	Engine sound	Silence	Relaxing tune	Silence	Crowd noise

In order to facilitate a comparative analysis of the results, the participants were provided with a questionnaire designed to capture their perception of the auditory stimuli: subsequent to the data collection process, a rigorous anonymization procedure was implemented to ensure the privacy and confidentiality of the participants.

The participants were then directed to use their smartphones to scan a QR code, which led them to an online questionnaire created using Google Form. This questionnaire was designed to collect a range of personal information from each participant, including their first name, last name, age, gender, country of origin, and the volume value set on the computer for the test.

These questions were organized into three sets, each containing three questions to be answered immediately after the conclusion of each audio segment. The questions were designed to gauge the participants' perception of the auditory stimuli, specifically in terms of how annoying or pleasant, relaxing or stressful, and quiet or loud they found each particular audio segment.

A consent form was given for privacy, confidentiality, and information purposes about ECO DRIVE - Development of innovative lightweight and highly insulating energy efficient components and associated enabling materials for cost-effective retrofitting and new construction of curtain wall facades.
ECO DRIVE is a research project to develop new technologies for the testing and simulation of eco-powertrains. The project offers a multi-disciplinary research-training program to Early-Stage-Researchers, with the ultimate aim being to create a new generation of NVH professionals for the transport sector. ECO DRIVE deals with the complex challenges related to combustion noise, the irritating sound from electric motors, transmission induced NVH (Noise, Vibration and Harshness) and driveline torsional vibrations, leading to new designs with improved eco-efficiency and NVH performance.

The EEG signal was recorded by Muse Monitor sensors and recording device and 4 different electrodes were employed in the acquisition: two placed on the temporal lobes (TP9 and TP10) and two on the frontal lobe (AF7 and AF8), achieved to be subsequently elaborated using MATLAB and EEGLAB.

5.2 Muse Monitor sensors and recording device

Muse Monitor is an EEG measurement system consisting of:

1. An EEG device for the acquisition of EEG signal, see Figure 5.2
2. a mobile app designed by Muse that enables real-time monitoring and recording of electroencephalogram (EEG) signals while wearing a custom EEG headset. The app is available for iOS and Android devices and uses Bluetooth Low Energy (BLE) technology to interface with the mobile device, processing signals and displaying brain activity on the device's screen.

The system provides users with rapid feedback and enables them to see how it changes in response to various stimuli or cognitive activities. [5.3]

Figure 5.2 The 2016 Muse EEG system made by InterAxon Inc [5.4]

The arrangement of electrodes adhered to a specific protocol. The reference electrode, designated as FPz, was strategically positioned on the forehead. The input electrodes, identified as AF7 and AF8, were composed of silver and were situated on the left and right sides of the reference, respectively. In addition, two posterior electrodes, TP9 and TP10, were affixed above each ear, utilizing conductive silicone-rubber material. Prior to the placement of the headband on the subjects' heads, the skin at the electrode sites was meticulously cleaned with alcohol swipes, and a thin layer of water was applied to the electrodes using a sponge to enhance the quality of the signal. The MUSE device captured signals at a sampling frequency of 256 Hz.

Muse Monitor also allows to record and archive EEG sessions for future further investigations. The program, in fact, could be used in conjunction with a variety of third-party solutions as biofeedback software, games, or other applications that utilise EEG input. Muse Monitor can thus be used as an input device to control various user interfaces or to build interactive experiences based on brain activity. The program includes extensive analytics tools to measure and assess the documented brain activity during recording. For example, it is able to calculate EEG frequency bands such as delta, theta, alpha, beta, and

gamma and present them in clear, easy-to-understand graphs. This study, known as power spectrum density, allows to determine which type of frequency band is dominant at any given time or in reaction to a certain stimulus and can reveal more information about patient's consciousness [5.3].

Muse Monitor also allows to customise the Muse headset's settings, such as increasing the sensitivity of the sensors and electrodes or modifying the time of recording sessions. These options enable to personalise the gadget to the user's individual needs and achieve more precise and dependable results.

5.3 EEGLAB

EEGLAB is an advanced, high-level, and interactive toolbox that has been designed for the MATLAB environment. Its primary purpose is to facilitate the comprehensive processing of continuous and event-related Electroencephalogram (EEG), Magnetoencephalography (MEG), and other forms of electrophysiological data.

The toolbox is complex in its structure, embodying a multitude of features that cater to a wide array of needs in the field of electrophysiological data analysis. One of its key features is the implementation of Independent Component Analysis (ICA), a statistical technique used to separate a multivariate signal into additive subcomponents.

In addition to ICA, EEGLAB also incorporates time/frequency analysis, a method used to examine the temporal evolution of spectral power in different frequency bands. This feature is particularly useful in the study of oscillatory brain activity.

Artifact rejection is another significant feature of EEGLAB. This functionality allows users to identify and remove various types of noise and artifacts from the electrophysiological data, thereby enhancing the accuracy of the results.

Furthermore, EEGLAB provides capabilities for conducting event-related statistics. This feature enables users to perform statistical analyses on event-related potentials (ERPs),

which are brain responses that are directly the result of a specific sensory, cognitive, or motor event.

Lastly, EEGLAB offers several useful modes of visualization for both averaged and single-trial data. These visualization tools provide users with the means to effectively examine and interpret their data, thereby facilitating a deeper understanding of the underlying neural processes. [5.5] [5.6]

The software provides an interactive graphical user interface (GUI), enabling users to process high-density EEG and other dynamic brain data in a flexible and interactive manner. It supports the use of independent component analysis (ICA) and/or time/frequency analysis (TFA), as well as standard averaging methods. EEGLAB also incorporates extensive tutorial and help windows, plus a command history function that eases users' transition from GUI-based data exploration to building and running batch or custom data analysis scripts. [5.5] [5.6]

When associated with Matlab, EEGLAB offers a structured programming environment that allows for the storage, access, measurement, manipulation, and visualization of event-related EEG data. It also provides an extensible, open-source platform that enables them to share new methods with the global research community by publishing EEGLAB 'plug-in' functions that appear automatically in the EEGLAB menu of users who download them. For example, novel EEGLAB plug-ins might be built and released to 'pick peaks' in ERP or time/frequency results, or to perform specialized import/export, data visualization, or inverse source modeling of EEG, MEG, and/or ECOG data. [5.5] [5.6]

In this study, to avoid having to load and work with datasets one at a time, a specific function for importing data, '*pop_musemonitor*', was extracted from a specific open-source plug-in. This function was used to import data acquired exclusively with the Muse Headband, enabling the creation, work with, and customization of a script in MATLAB. The '*pop_musemonitor*' function not only allowed the import of data acquired with the Muse Headband but also facilitated an initial clean-up of the data thanks to the automatic process performed by the plug-in. In particular, several parameters were set: the sampling rate, checkboxes that allowed cleaning bad channels and data corrupted by artifacts with their

respective thresholds, and finally a first high-pass filter with a frequency of 0.5 Hz, as reported in Figure 5.3.

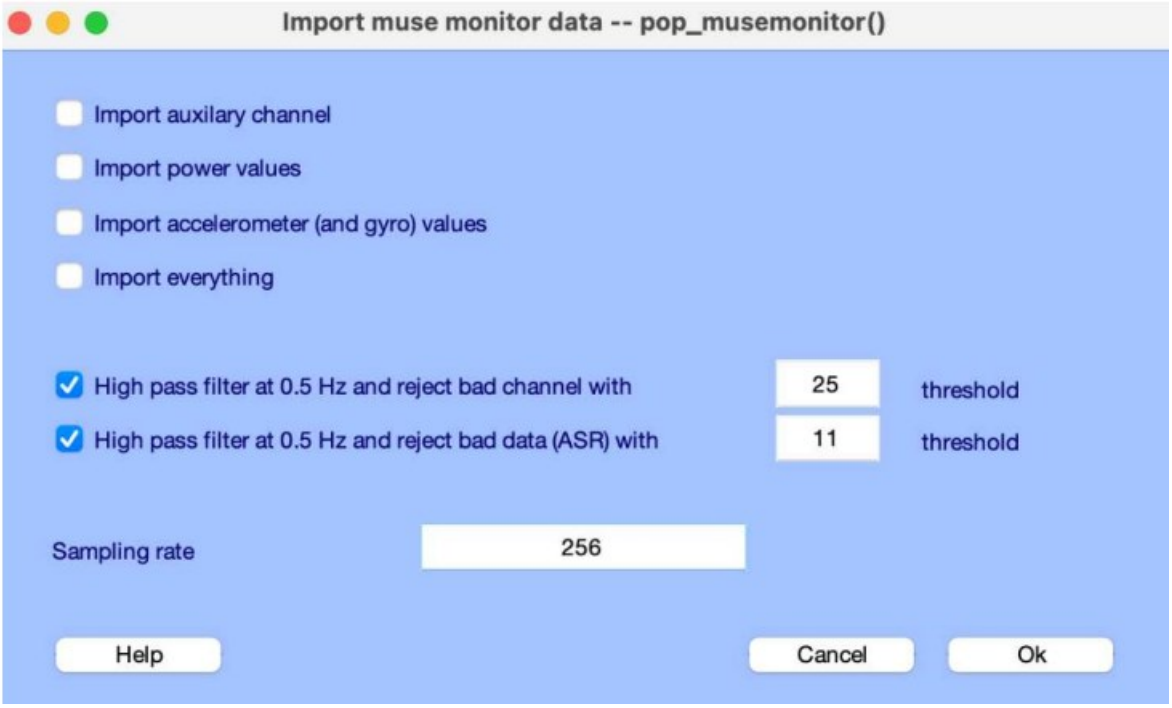

Figure 5.3 GUI window in EEGLAB Toolbox that allow to import .CSV file recorded with Muse Headband Device.

CHAPTER 6 – Data processing

Following the recording of the various EEG signal samples, they were divided by subject and according to the event in progress during the acquisition. Three different methods to observe the signals were compared: Muse Monitor autocleaning EEGLAB plugin, that was designed specifically for the used instrumentation, raw signal elaboration, and Autoreject algorithm, an automated artifact impacted signal dismissal for MEG and EEG data.

6.1 Muse Monitor autocleaning

During the empty dataset deleting step, the number of participants was reduced from 44 to 40, and, after using the Muse Monitor cleaning function, the 37 subjects temporal lobe signals were preserved, while the frontal lobe signals were almost entirely deleted. Then, to better visualize the signals, the power spectrum density was computed using the MATLAB function "*pwelch*". The Welch method is based on the idea of estimating power spectral density (PSD) from a signal that has been converted from the time domain to the frequency domain. Welch's method improves on the classic spectral density estimation method by lowering noise in the calculated power spectra. Noise reduction from Welch's approach is frequently required due to the noise created by imprecise and finite data (Welch 1967). The method separates the time series into (potentially overlapping) segments before calculating a modified spectrogram for each segment and averaging the PSD estimates. When compared to a single spectrogram estimate of the whole data record, this strategy reduces the variation of the estimate. However, this strategy reduces the estimator's resolution, implying that there is a trade-off between variance reduction and frequency resolution. In this work, we utilised 50% overlapping Hann tapers of 0.5 s to estimate the PSD in both theta and beta frequency ranges for the Welch's technique analysis [6.1].

The power spectrum density related to the frontal lobe, AF7 and AF8, were heavily discarded by the function, so it was impossible to compute the following steps and obtain enough data to proceed with the parameters calculation, while the number of the subjects with both TP9 and TP10, using the temporal lobe electrode signals, lowered to 37. The PSD of the TP9 electrode is reported in Figure 6.1 (cleaned data) and in Figure 6.2 (raw data). The PSD of the TP10 electrode is reported in Figure 6.3 (cleaned data) and in Figure 6.4 (raw data).

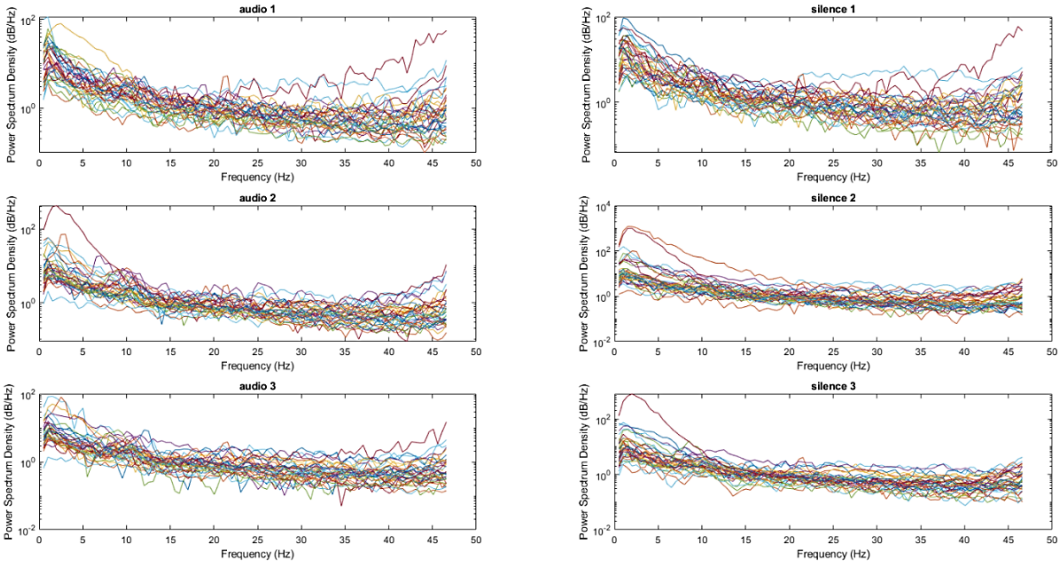

Figure 6.1 TP9 electrode Power Spectrum Density image using Muse Monitor autocleaning function.

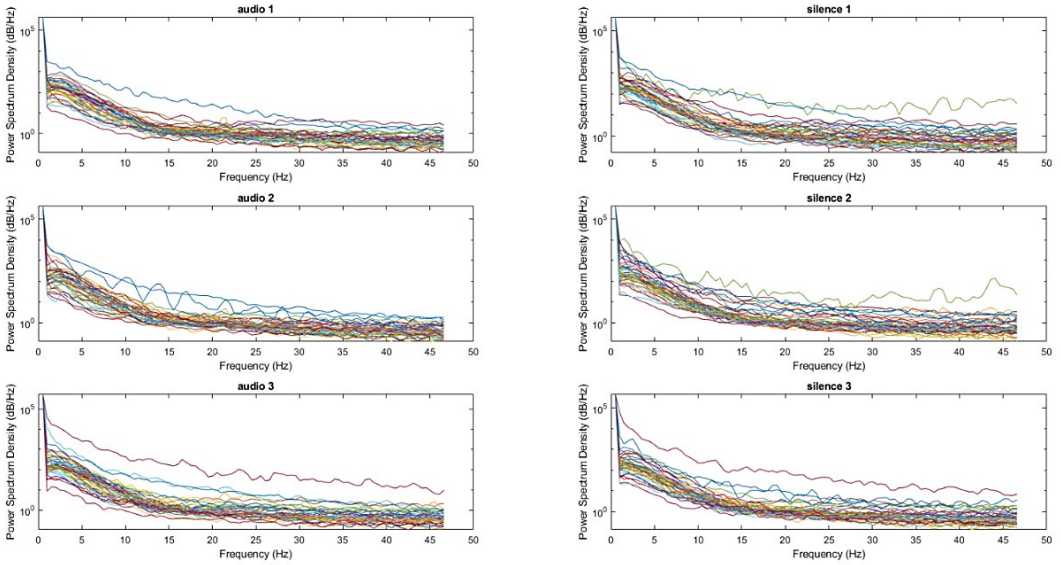

Figure 6.2 TP9 electrode Power Spectrum Density image using raw data.

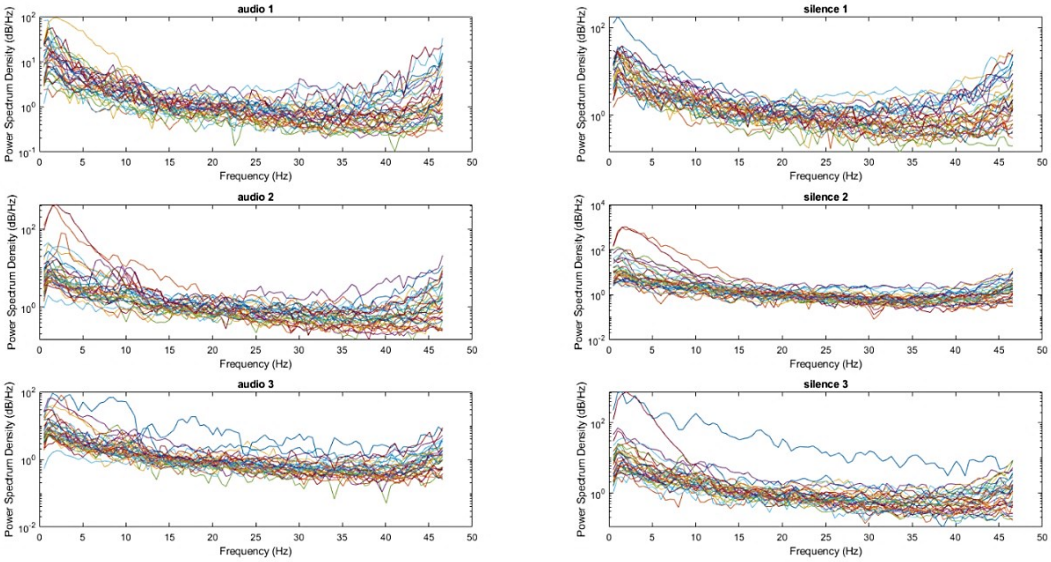

Figure 6.3 TP10 electrode image using Muse Monitor autocleaning function.

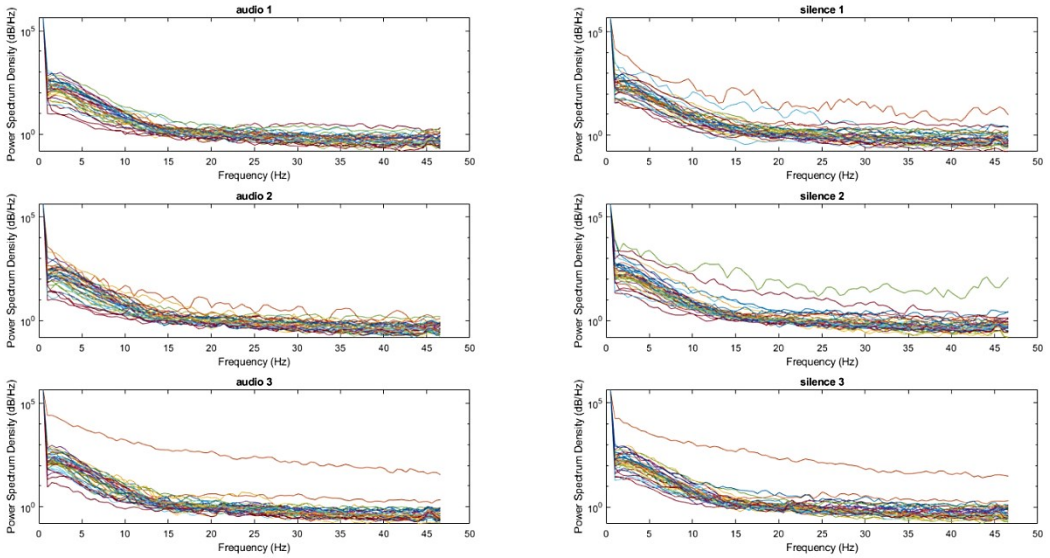

Figure 6.4 TP10 electrode Power Spectrum Density image using raw data.

To get a better understanding of the trend that is present when the subject is experiencing different emotions, for example different stress or involvement levels, by the various frequency waves content, it was important to remove the outliers, that can be caused by different kinds of error during the acquisitions and can significantly change the presumed

power spectrum density of frequency bands. The function involved was "*rmoutliers*". The PSDs remaining after the outliers removal are shown in Figure 6.5 and Figure 6.7, for TP9 and TP8 respectively. The outliers removal has been done also for the PSD calculated from the raw data: see Figure 6.6 and Figure 6.8.

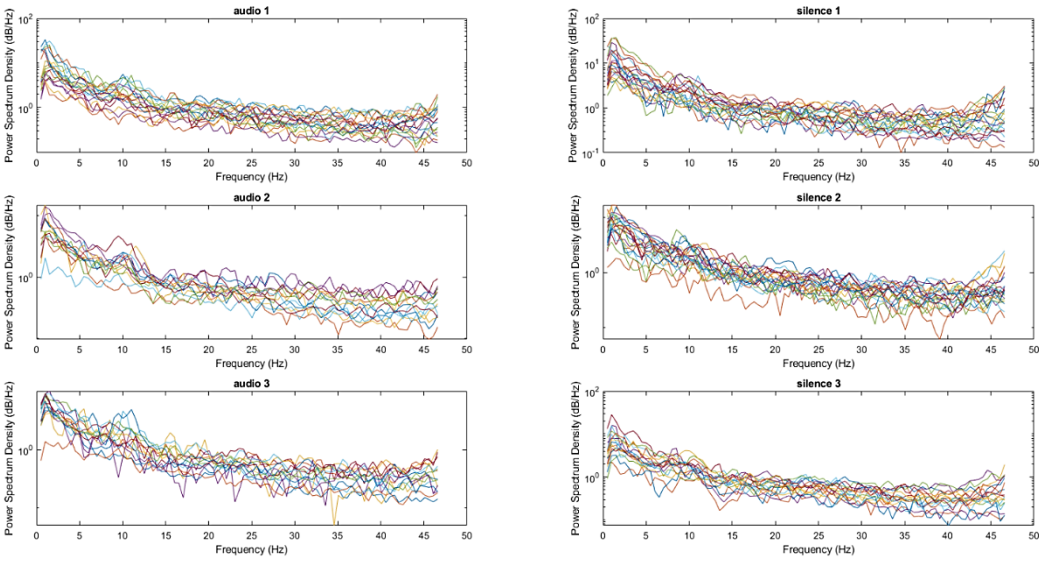

Figure 6.5 TP9 electrode Power Spectrum Density image using Muse Monitor autocleaning function.

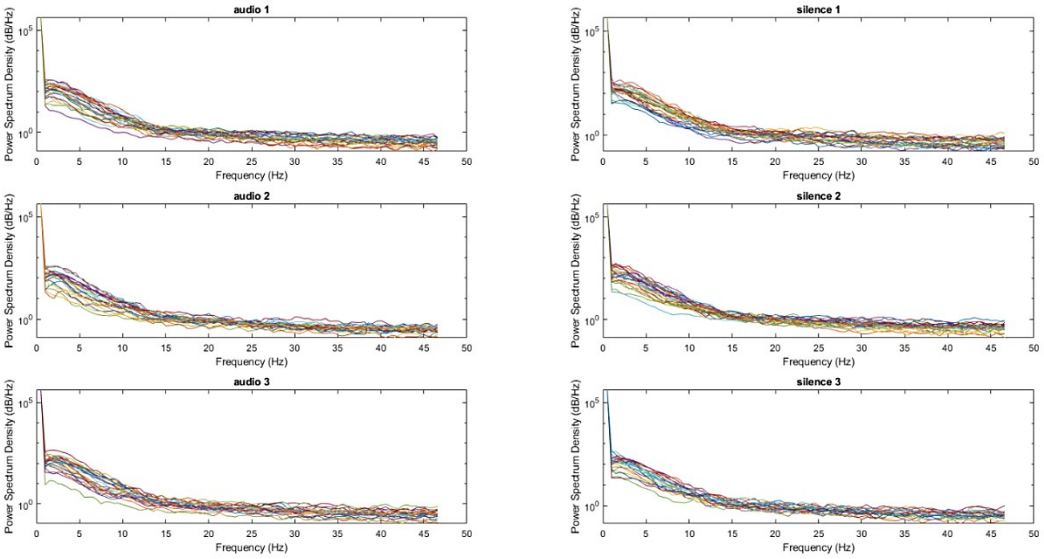

Figure 6.6 TP9 electrode Power Spectrum Density image using raw data

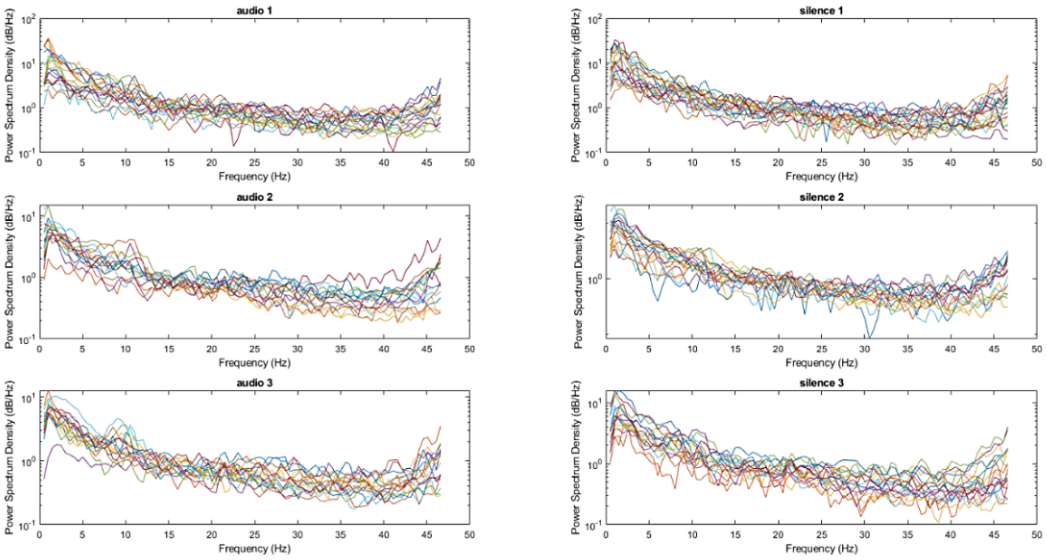

Figure 5.7 TP10 electrode Power Spectrum Density image using Muse Monitor autocleaning function.

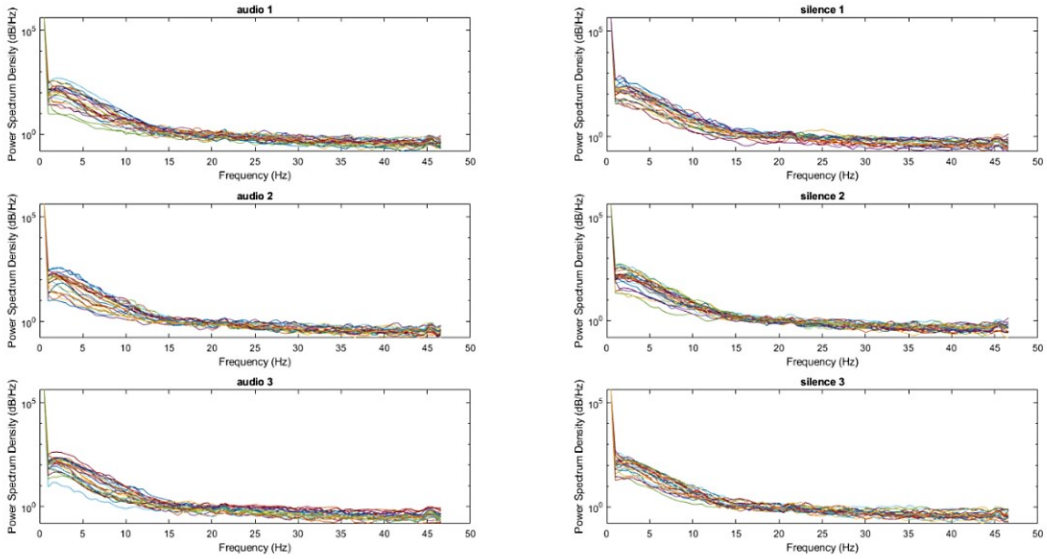

Figure 5.8 TP10 electrode Power Spectrum Density image using raw data.

Some limitations of this signal cleaning process can be attributed to excessive removal during the process, which can lead to information and accuracy loss, not only in frontal lobe signals but also in the temporal lobe ones. Some were reduced to slightly more than 5

seconds while the original time window was 60 seconds long. Figure 5.9 reports two examples of TP9 time histories registered from two different subjects (subject n. 8 and n. 37) while listening to audio 3 and cleaned with the Muse Monitor autocleaning function. It is clear that the signal cleaned for subject 8 has been strongly affected. The remaining part was only 5 seconds long. On the other hand, the cleaning for signal from subject 37 was less invasive, since its length remains of about 40 seconds.

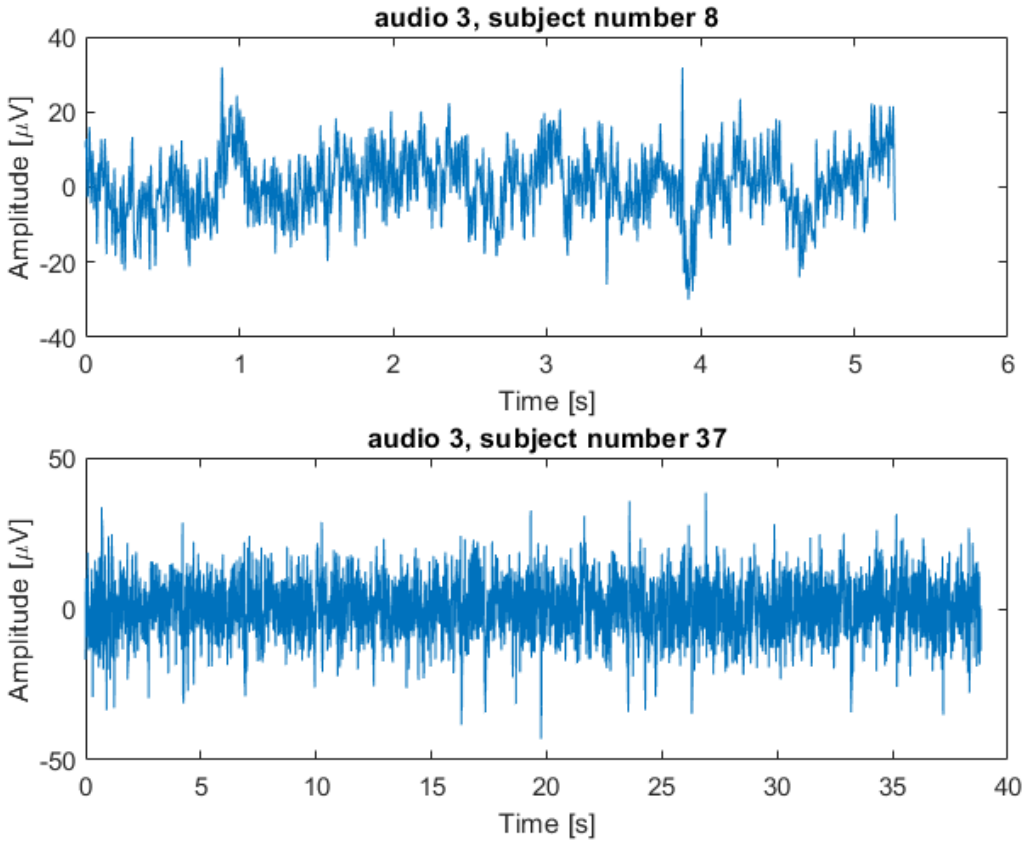

Figure 6.9 TP9 time history after Muse Monitor autocleaning function use.

6.2 Autoreject algorithms

The autocleaning implemented inside the Muse Monitor was too invasive, as demonstrated in the previous paragraph (for instance the signal coming from the AF electrodes were completed removed). For this reason, the EEG signals have been cleaned with an autoreject algorithm implemented directly in Matlab. In this case the signal cleaning was less invasive.

The shortest segment of the cleaned signals was of 2565 samples, which corresponds to about 10 seconds at 256 Hz sampling frequency. In order to perform a coherent analysis of all the signals. Clean data analysis was performed using the last 10 seconds of each sample, as the brain takes some time adjusting to the new information and the emotional reaction is delayed in time [6.2]. Working only on this timeframe gives us to have more clean-cut values to work on for the parameters of interest for the analysis of the reaction of these 3 stimuli.

Starting from these samples, the Power Spectrum Density was calculated using the "*pwelch*" function implemented in Matlab.

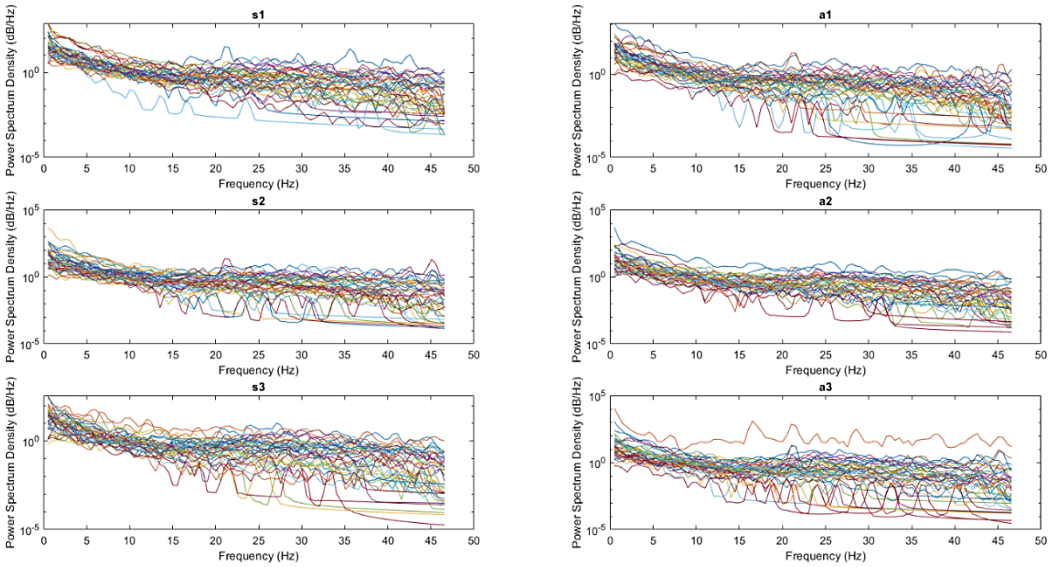

Figure 6.10 Power Spectrum Density divided by time segment (3 audio stimuli execution and 3 silences alternated to them) for AF8.

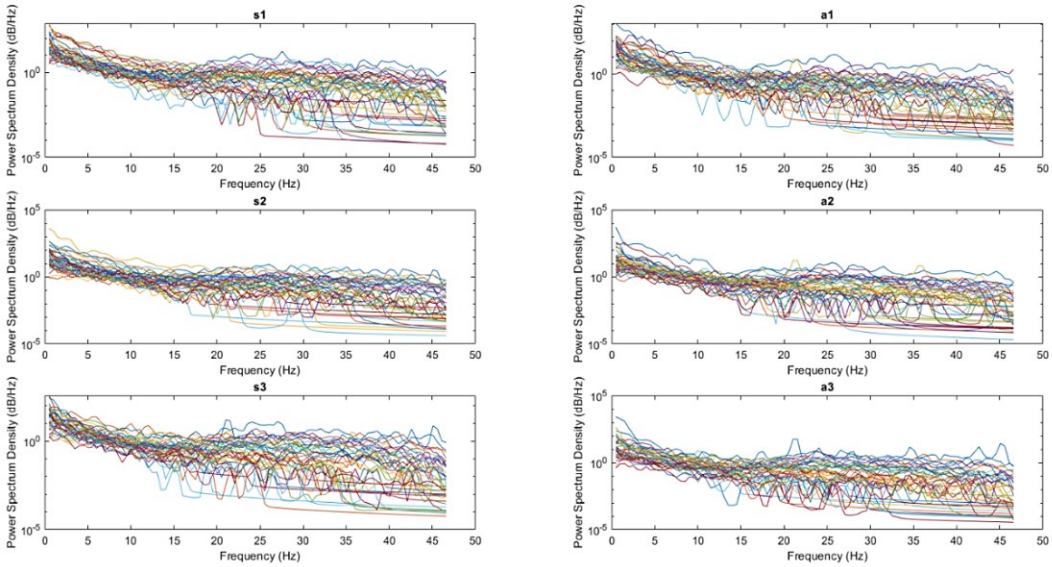

Figure 6.11 Power Spectrum Density divided by time segment (3 audio stimuli execution and 3 silences alternated to them) for AF7.

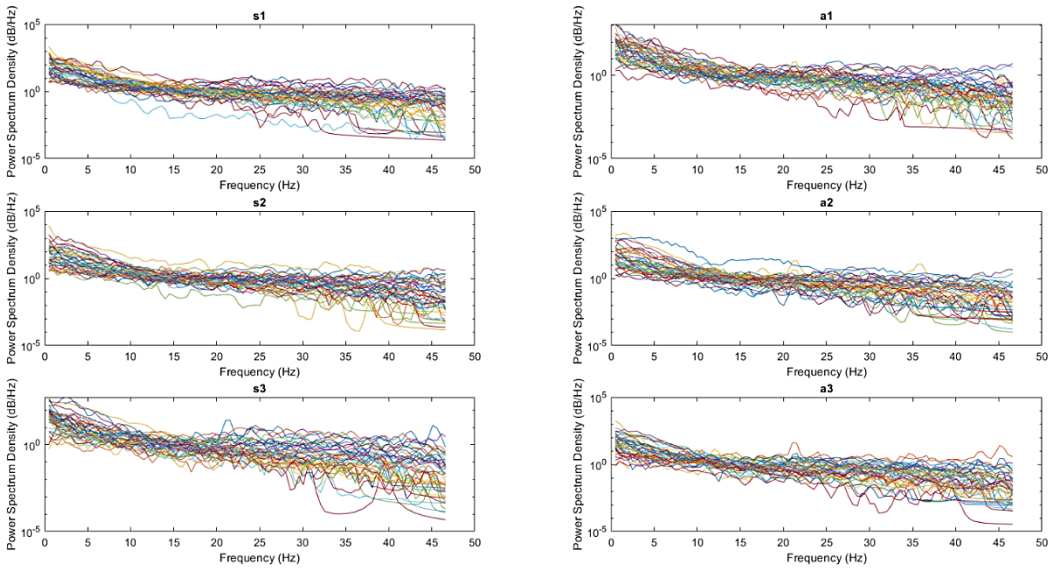

Figure 6.12 Power Spectrum Density divided by time segment (3 audio stimuli execution and 3 silences alternated to them) for TP9.

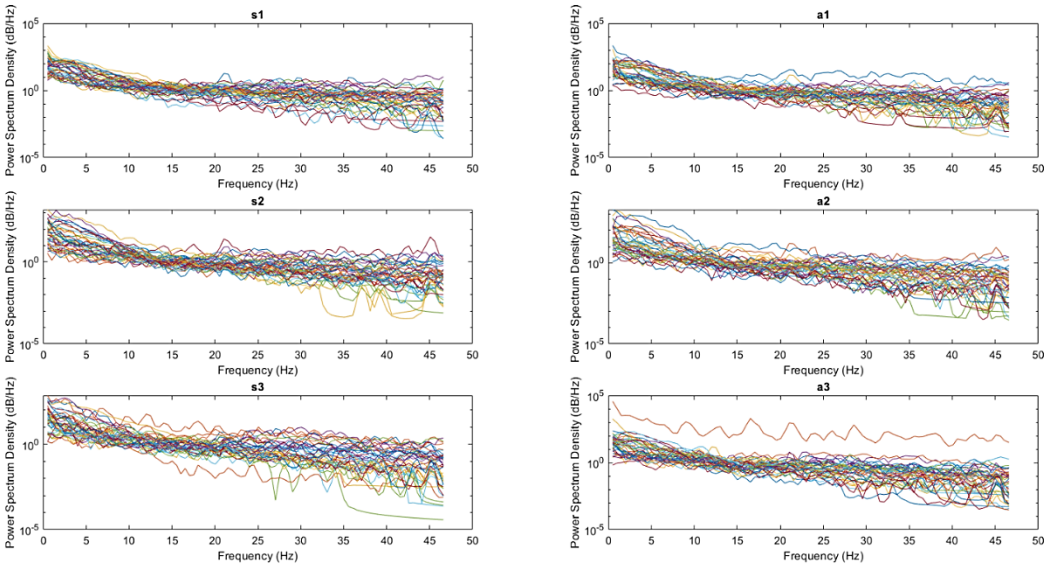

Figure 6.13 Power Spectrum Density divided by time segment (3 audio stimuli execution and 3 silences alternated to them) for TP10.

In this case the outlier removal has not been done on the PSD, but directly on the extracted features, specifically on the alpha wave frequency band, theta-beta ratio, and alpha-beta ratios.

6.3 Features calculation

6.3.1 Alpha wave

Alpha band frequency wave, that comprehends the range between 8 and 13 Hz, has been filtered for each subject in the 6 different cases, and the dataset cleaning has been restricted to this interval using the function "*rmoutliers*" as, cleaning the dataset before selecting the intended frequency range, could have been limiting for the purpose.

A mean value has been identified for each sample using the '*rms*' function on Matlab, as the root mean square function was the chosen method to identify a single alpha band frequency value for each case with the related standard error (Figure 6.14 and 6.15).

The Root Mean Square (RMS), also known as the quadratic mean, is a statistical measure of the magnitude of a varying quantity. In details, the RMS of a set of numbers is defined as

the square root of the mean square (the arithmetic mean of the squares) of the set. For a set of n numbers or values of a discrete distribution x_i, ..., x_n, the RMS is the square root of the mean of the values x_i^2, namely:

$$X_{RMS} = \sqrt{\frac{x_1^2 + x_2^2 + \cdots + x_n^2}{n}} = \sqrt{\frac{\sum_{i=1}^{n} x_i^2}{n}}$$

In estimation theory, the root-mean-square deviation of an estimator is a measure of the imperfection of the fit of the estimator to the data.

The term "Standard Error" (SE), instead, is employed to quantify the precision with which a sample epitomizes the underlying population. The standard error is essentially the standard deviation of the sampling distribution of a statistic. When the statistic in question is the sample mean, the term "Standard Error of the Mean" (SEM) is used.

The standard error serves as a fundamental component in the construction of confidence intervals. It provides an estimate of the degree of variation one might expect in the sample mean, should the study be replicated with new samples drawn from the same population. This measure of variability is instrumental in gauging the reliability of the sample mean as an estimator of the true population mean, thereby justifying its use in this research.

The formula for the standard error of the mean is:

$$SE = \frac{\sigma}{\sqrt{n}}$$

where:

- σ is the standard deviation of the population,
- *n* is the size (number of observations) of the sample.

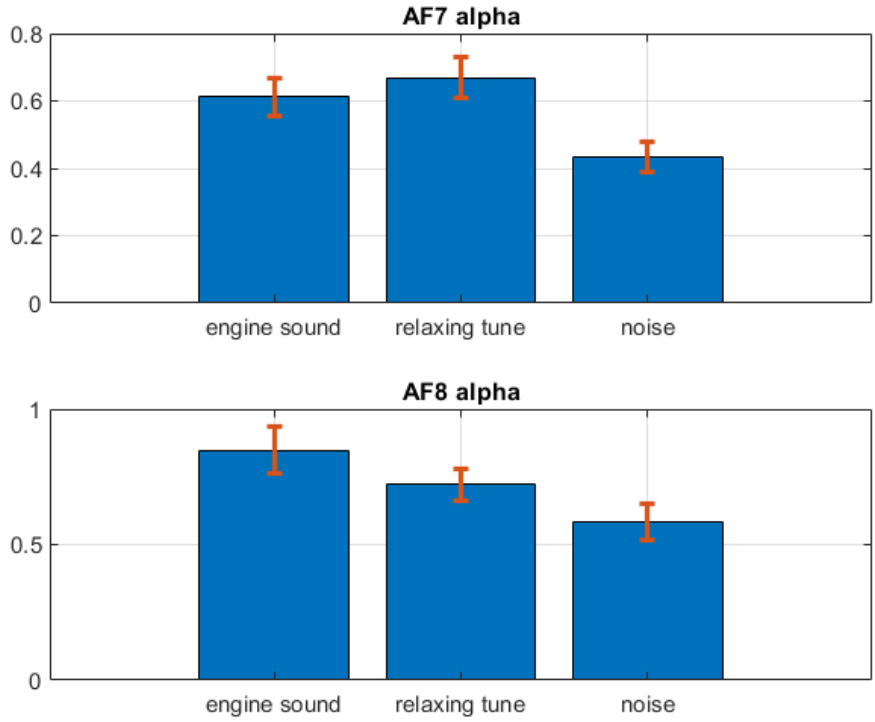

Figure 6.14 alpha frequency band mean value for each case for AF7 and AF8 electrodes, with standard error.

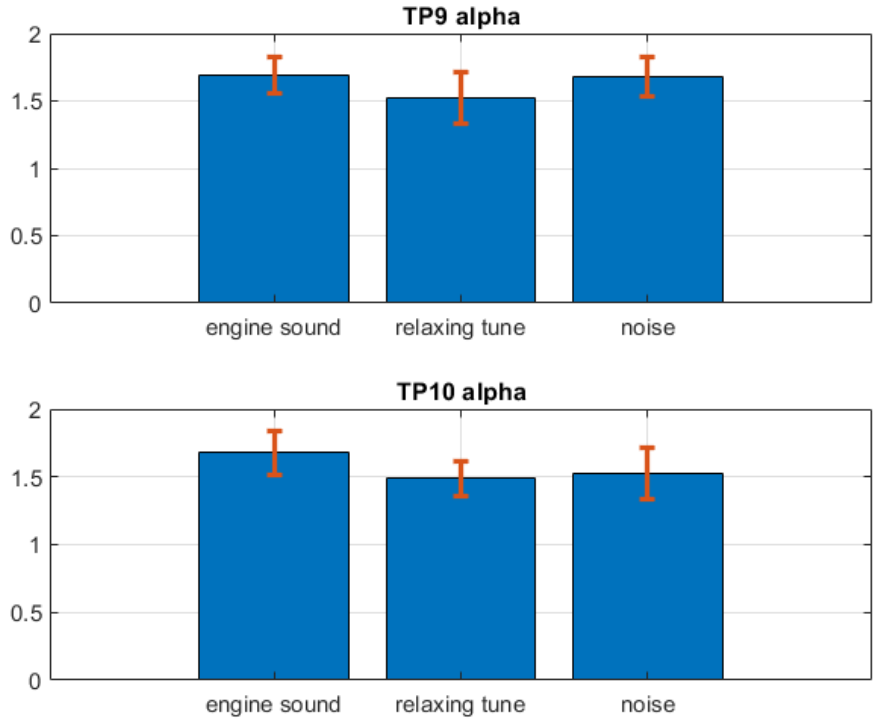

Figure 6.15 alpha frequency band mean value for each case for TP9 and TP10 electrodes, with standard error.

6.3.2 Alpha-beta ratio

Same process applied in the calculation of Alpha wave can be applied for Beta frequency band sample rate (Figure 6.16 and 6.17) to visualize a mean value for the 3 different sensory input cases, ±SE, the standard error. Beta waves, as previously stated, are a type of neural oscillations, or brainwaves, that have a frequency range of between 12.5 and 30 Hz (12.5 to 30 cycles per second).

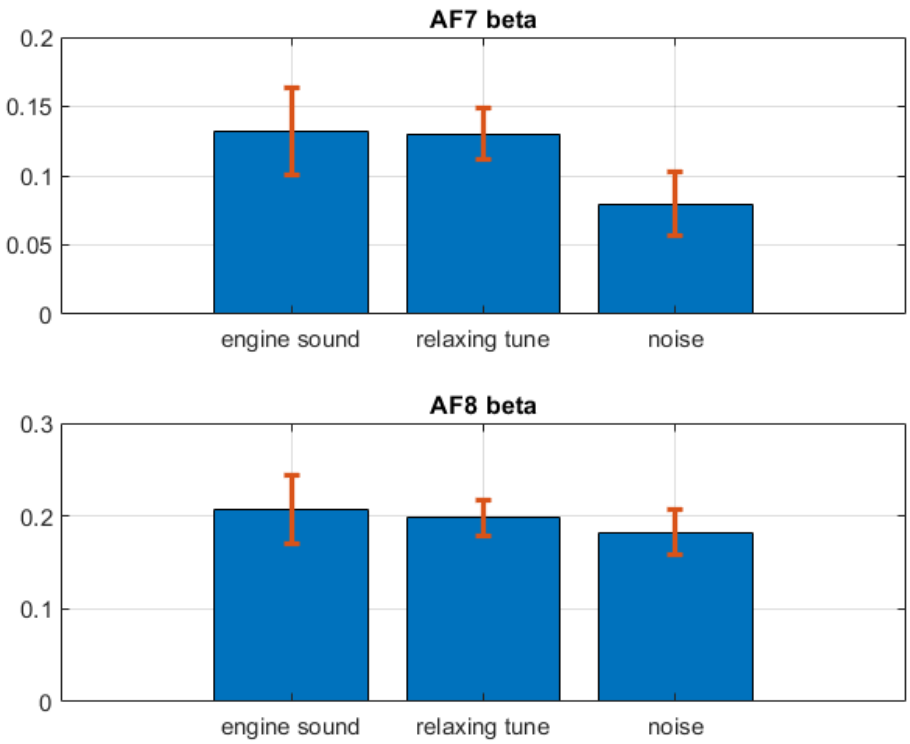

Figure 6.16 beta frequency band mean value for each case for AF7 and AF8 electrodes, with standard error.

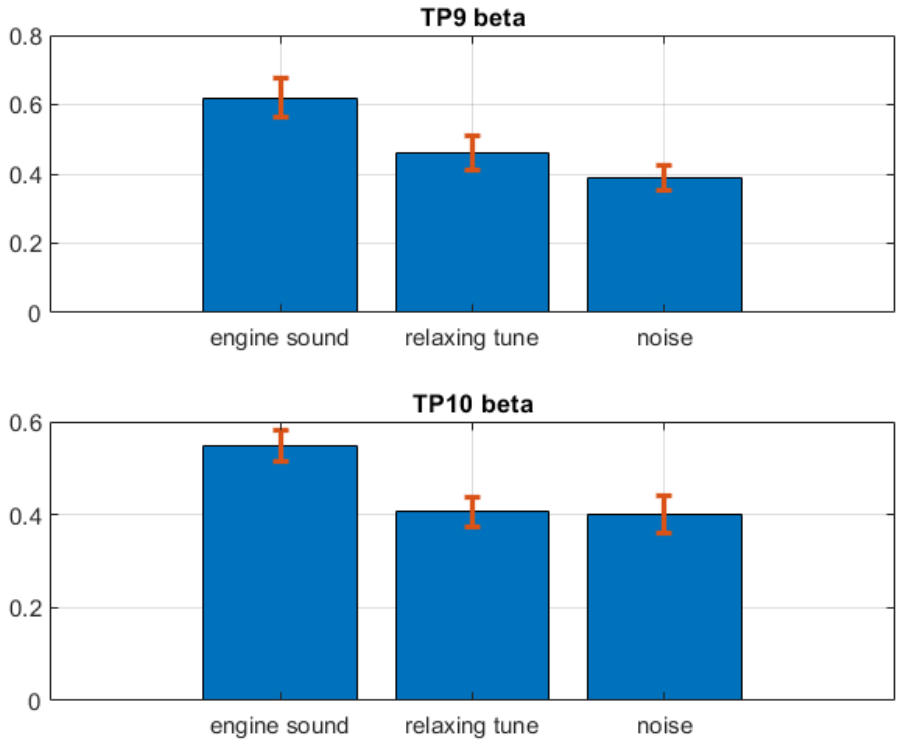

Figure 6.17 beta frequency band mean value for each case for TP9 and TP10 electrodes, with standard error.

In the computation of the alpha-beta ratio, the methodology employed for the preceding frequency wave was similarly applied to the Beta band range. The '*rms*' function was utilized to ascertain a singular value for both the Alpha and Beta bands. Subsequently, the ratio function was employed to analyse the difference in spectral power values for each subject, thereby facilitating an observation of its variation across three distinct audio inputs.

The data set was then segregated from the outlier using the '*rmoutliers*' function. The data identified as outliers were flagged for elimination, effectively removing the entire data set corresponding to that subject. This measure was implemented to circumvent potential complications associated with movement artifacts or other issues linked to the acquisition procedure and the device. Figures from 6.18 and 6.19 show the alpha/beta ratio for the different sounds at the different electrodes.

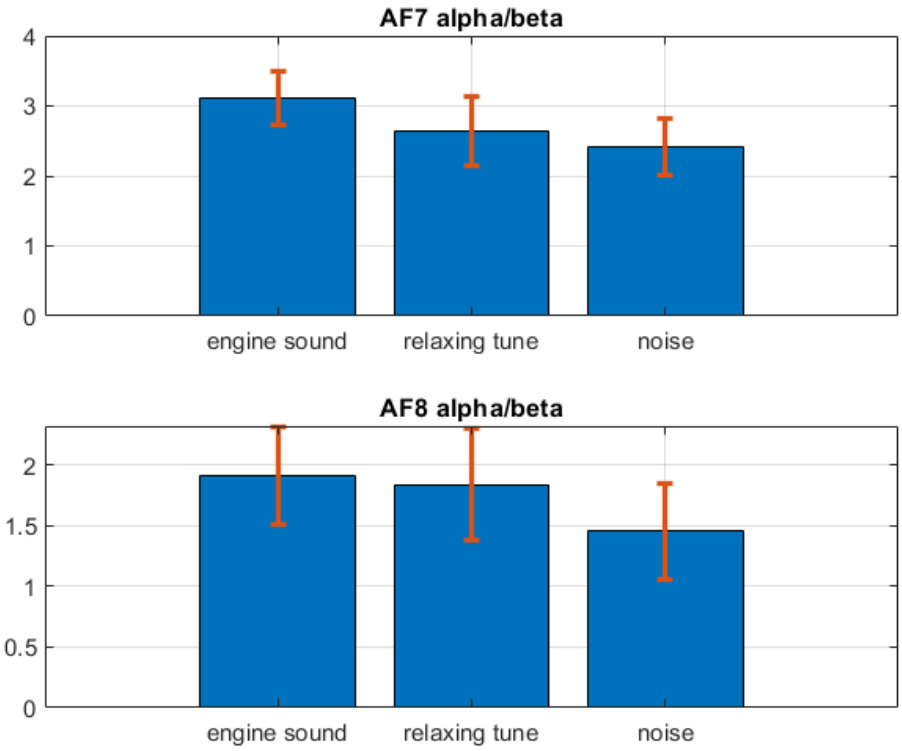

Fig 6.18 Alpha-Beta ratio calculated for frontal lobe electrodes (AF7 and AF8) with standard error

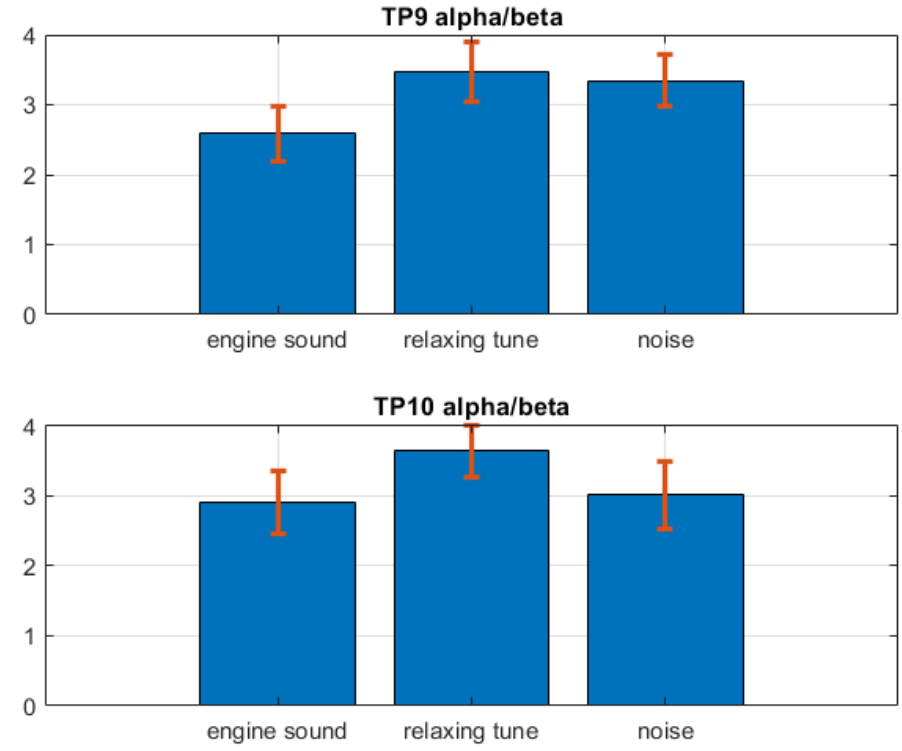

Fig 6.19 Alpha-Beta ratio calculated for temporal lobes electrodes (TP9 and TP10) with standard error

6.3 Theta-Beta Ratio

In order to calculate the theta-beta ratio, the exact same methodology as employed for the previous frequency wave parameters was applied to the Theta band range (Figure 6.20 and 6.21). The ‘rms’ function was utilized to ascertain a singular value for both the Theta and Beta bands. Subsequently, the ratio function was employed to compare the spectral power value differences for each subject, thereby facilitating an observation of how it varies across three distinct audio inputs.

The data set was subsequently separated from the outliers using the ‘rmoutliers’ function. The data identified as outliers were flagged for deletion, effectively removing the entire data set corresponding to that subject. This measure was taken, again, to circumvent potential issues associated with movement artifacts or other complications linked to the acquisition procedure and the device. The theta/beta ratio for the different sounds at the different electrodes are shown in Figure 6.22 and Figure 6.23.

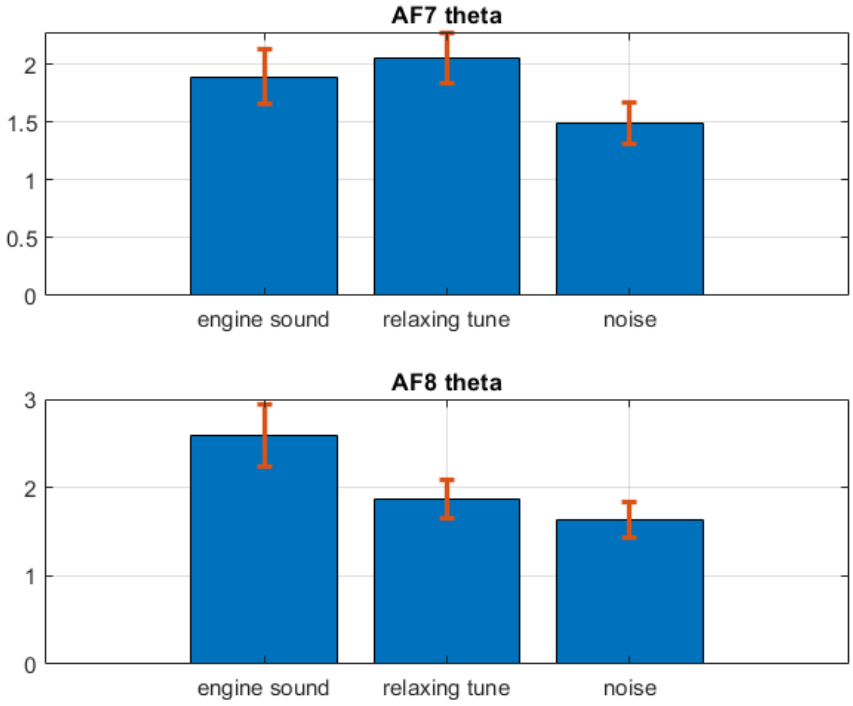

Figure 6.20 theta frequency band mean value for each case for frontal lobe electrodes (AF7 and AF8) with standard error.

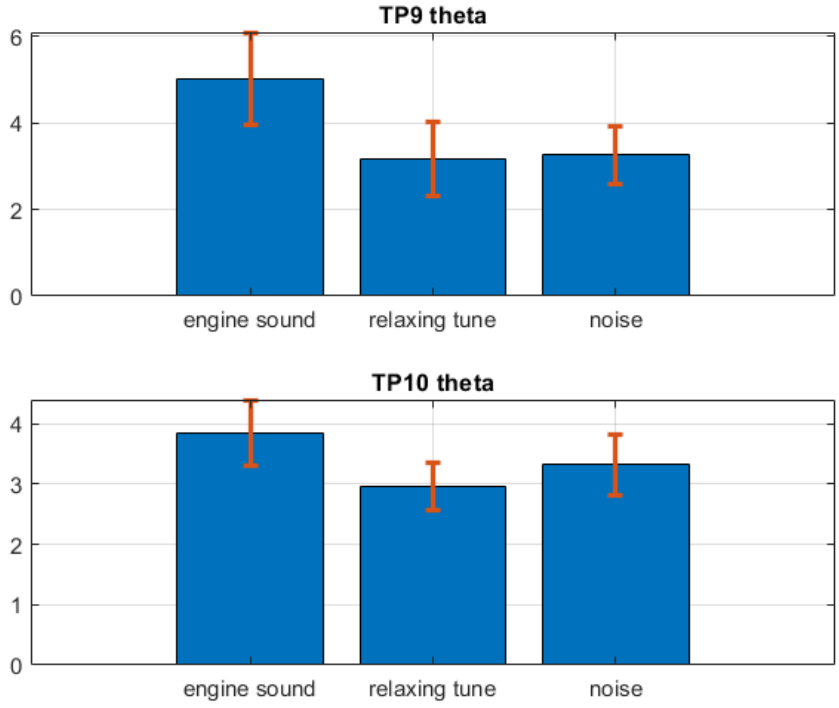

Figure 6.21 theta frequency band mean value for each case for temporal lobes electrodes (TP9 and TP10) with standard error.

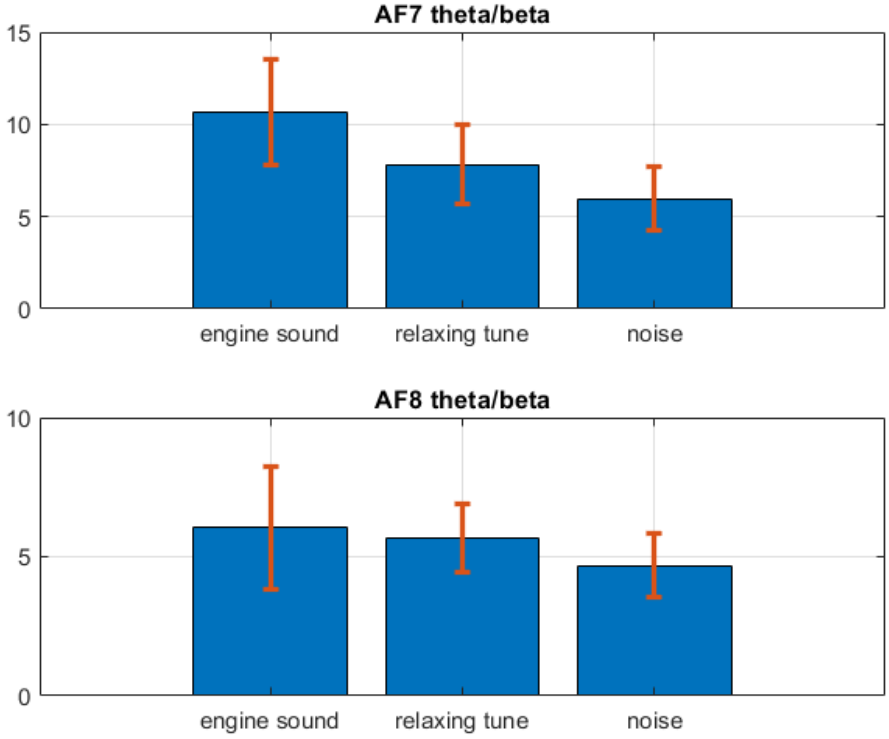

Figure 6.22 Theta-Beta Ratio for frontal lobe electrodes (AF7 and AF8) with standard error

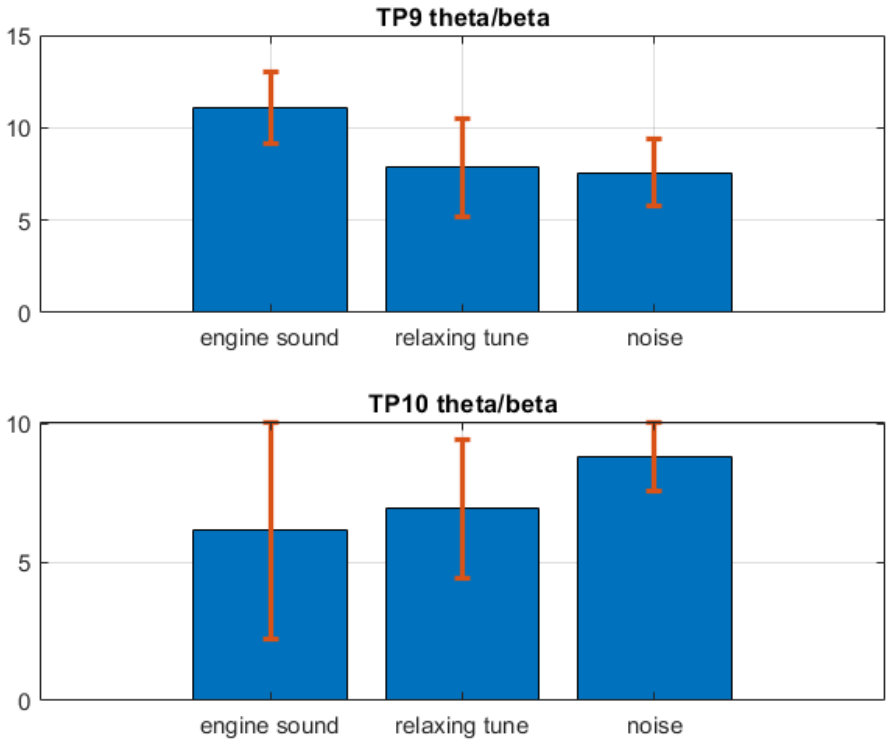

Figure 6.23 Theta-Beta Ratio for temporal lobes electrodes (TP9 and TP10) with standard error

6.4 Coherence analysis

The qualitative investigation of the signal features accuracy is significantly facilitated by the analysis of Coherence, between the left and the right hemisphere, which serves as a crucial and advantageous mathematical instrument.

The effectiveness of these methodologies is fundamentally anchored in the interaction, initially evidenced in 1995 [6.6], between the oscillations of the central and peripheral nervous systems, approximately at 20 Hz (so in the range of β band).

These studies have revealed the existence of communication mechanisms not only between the CNS and PNS but also within diverse structures of the brain itself, employing signals at varying frequencies contingent on the distance that the information is required to cover [6.7]. These interactions can exhibit substantial variations from one individual to another and are particularly noticeable in the presence of motor disorders such as Parkinson's disease or myoclonic epilepsy [6.8]. It suggests that while the coherence may be minimal in healthy subjects with excellent motor skills, its role in motor tasks is still significant.

During a hold-ramp-hold task, the coherence was found to be smaller under isometric conditions compared to compliant conditions, indicating a positive correlation between coherence strength and object compliance in the 15–30 Hz range. This suggests that corticomuscular coherence might be associated with specific parameters of hand motor function, potentially reflecting a functionally important process such as the recalibration of length-tension ratios. The study also discusses a study testing the effect of diazepam and its antagonist flumazenil on corticomuscular coherence. [6.8]

The coherence between two signals, denoted as x(t) and y(t) and interpreted as stochastic processes, is articulated in the frequency domain, bearing a resemblance to the form of the correlation coefficient. This mathematical representation underscores the profound interconnectedness and mutual influence between the two signals, thereby providing a robust framework for their comprehensive analysis:

$$Coh_{xy}(f) \triangleq \frac{P_{xy}(f)}{\sqrt{|P_x(f)|} \cdot \sqrt{|P_y(f)|}}$$

In which $P_x(f)$ and $P_y(f)$ are the Power Spectrum densities of, respectively, x and y, while $P_{xy}(f) = \frac{1}{n}\sum_{i=1}^{n} X_i(f)Y_i^*(f)$ is the Cross Power Spectral Density, CPSD.

The magnitude-squared coherence (MSC) [6.9], then, between the two one-dimensional wide-sense stationary signals x(t) and y(t) is defined as:

$$C_{xy}(f) \triangleq \left|Coh_{xy}(f)\right|^2 \triangleq \frac{\left|P_{xy}(f)\right|^2}{|P_x(f)| \cdot |P_y(f)|}$$

By the Cauchy–Schwarz inequality, as described in Malekpour et al. [6.9] this value is a real number between zero and one, for all frequencies *f* if and only if *x(t)* and *y(t)* are related through a linear time-invariant system, i.e., the two signals are linearly dependent over time.

Through this methodology, it becomes feasible to ascertain the degree of expected coherence divergence amongst the various signals, which are concurrently acquired from the same subject. This approach provides a robust framework for comprehending the intricate interplay of these signals and their potential variations. As it is possible to visualize in Figure 6.24, the electrodes on the left are AF7 and TP9, while the ones situated on the right part of the brain are AF8 and TP10.

On EEGLAB, the MSC function that is used to compute this is '*mscohere*'. Then, the Root Mean Square was again used to obtain a single value for each subject and the median of the subjects' value was computed to visualize the Coherence in a more efficient way, as seen in Figure 6.25 and 6.26.

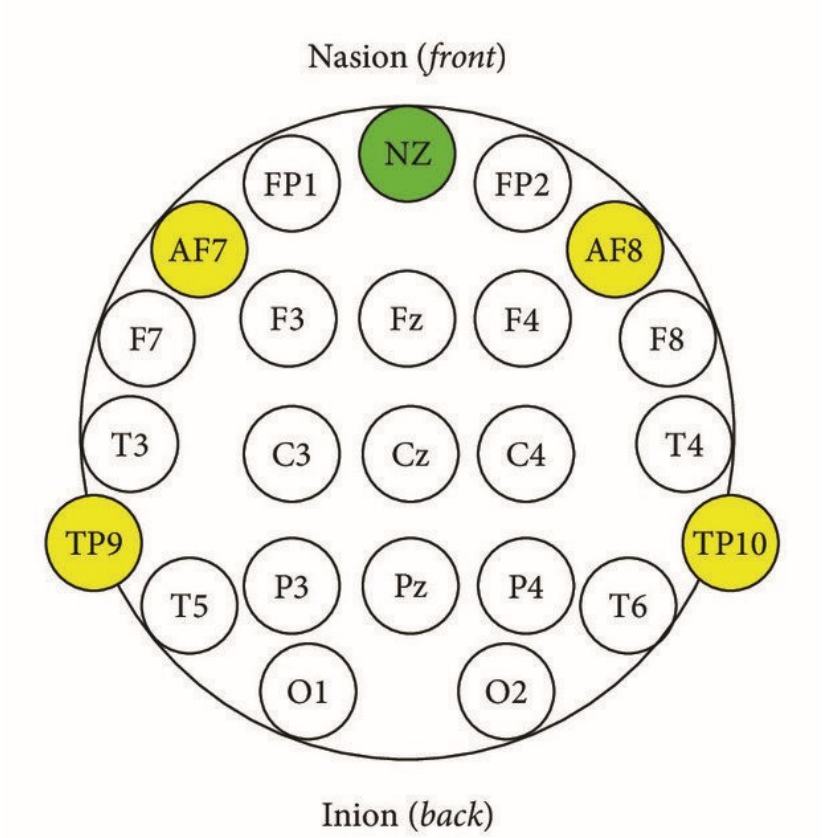

Figure 6.24 position of the 4 electrodes on the scalp: AF7 AF8 TP9 TP10

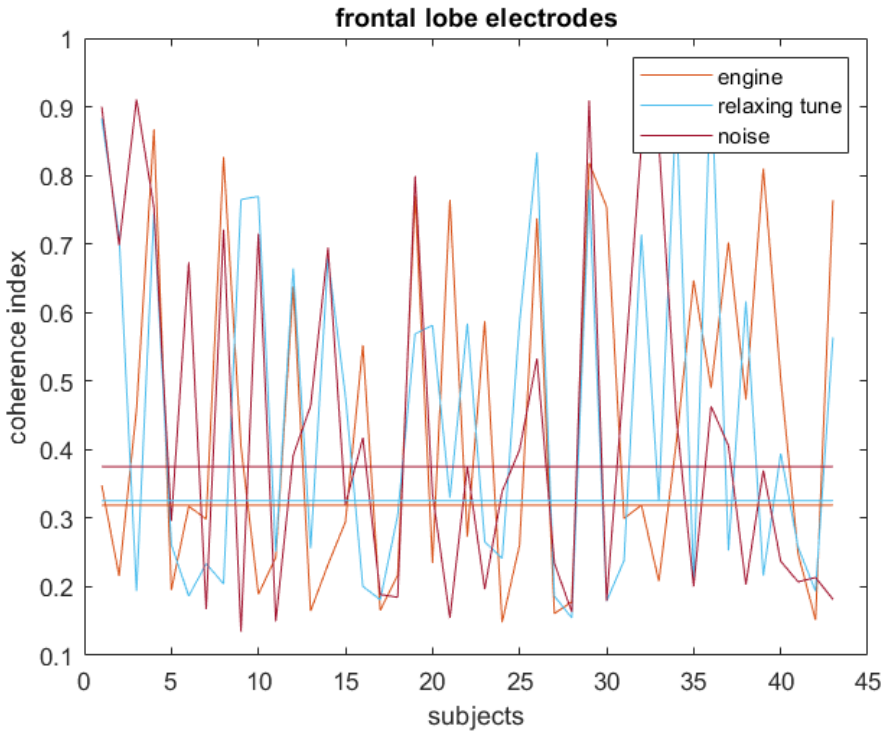

Figure 6.25 Coherence index for each subject between frontal lobe electrodes (AF7 and AF8), and mean of each Coherence index represented as continuous function

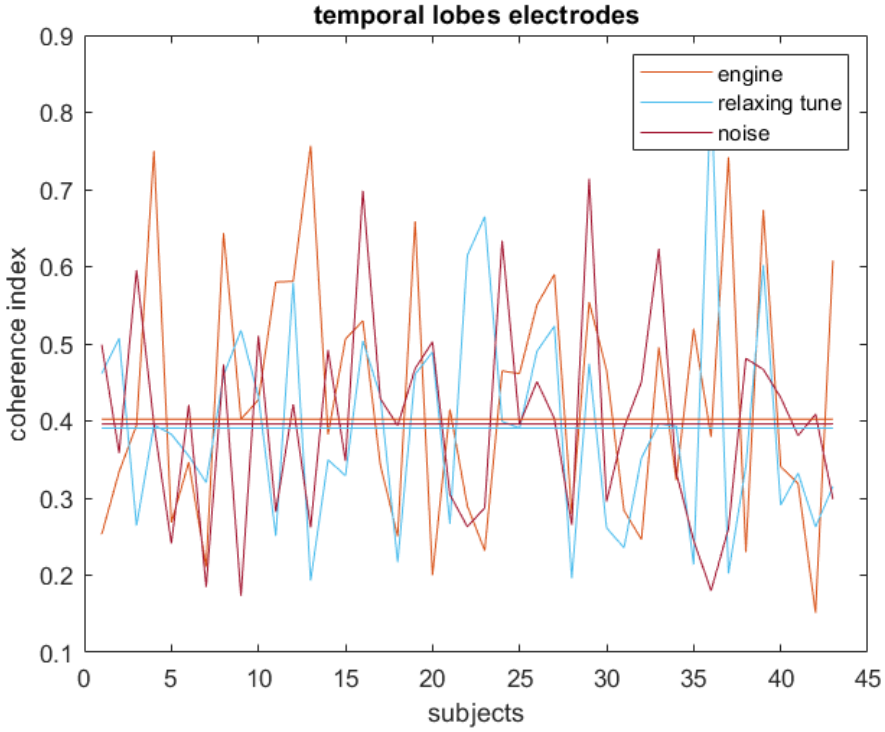

Figure 6.26 Coherence index for each subject between temporal lobes electrodes (TP9 and TP10), and mean of each Coherence index represented as continuous function

7. CONCLUSION

As illustrated in Figures 6.18 and 6.19, the alpha-beta ratio exhibits a significant elevation when the subjects are subjected to a relaxing tune in comparison to the crowd noise. This data implies an enhanced state of relaxation among the subjects.

Alpha waves are generally linked with a state of consciousness that transpires during periods of relaxation with eyes closed, excluding sleep. On the contrary, Beta waves are dominant during a state of normal consciousness, alertness, or active concentration.
Hence, a pattern suggestive of stress can be manifested by an escalation in power in the Beta band and a reduction in power in the Alpha band, particularly in the prefrontal cortex (PFC) [4.14]. The PFC is instrumental in regulating short-term memory, planning, and concentration. Consequently, these findings offer substantial insights into the physiological responses to diverse auditory stimuli.

Conversely, a decrease in the Theta/Beta ratio is indicative of an enhanced stimulus-driven attention, suggesting that the subjects possess a superior ability to concentrate. It is plausible that the Theta/Beta ratio could be effectively employed as an additional predictive measure in the investigation of stress and cognitive processing capacity since noise is well-knowingly a factor that increases stress and diminishes comprehension levels.
In everyday life, in fact, the damages are not limited to the increase in daily life stress: a too high background noise in a working environment – even if too low to cause problems to the auditory apparatus - can cause a decrease in noradrenaline or cortisol, thus leading to deficits in motivation level and problem-solving capacity [7.1]. On the long run, it also increases the likelihood of abandoning correct ergonomic and postural positions, increasing the risk of developing musculoskeletal disorders [7.1], an increase in the sense of fatigue [7.2], and damage to long-term memory due to disturbances in slow wave sleep quality [7.3].

The observed distinction between the results between both the frontal and temporal lobes is corroborated by the low Coherence index exhibited in both the electrodes of the frontal and temporal lobes. While predominantly, it can be confidently asserted that the alpha-beta ratio serves as a superior indicator of sensory response.

Future studies may wish to substantiate the hypothesis that the alpha-beta ratio and theta-beta ratio are parameters that can be manifested at more elevated values in individuals with neurodevelopmental disorders characterized with a higher sensory sensitivity, such as Autism Spectrum Disorder (ASD) and ADHD, and it may be beneficial to explore the potential involvement of certain pharmaceuticals, including stimulants and dopamine regulators, as they could potentially alleviate distress in instances of heightened sensory discomfort. This could potentially establish Electroencephalography (EEG) as a valid diagnostic instrument and a means to expand our knowledge on the matter in the future.

BIBLIOGRAPHY

CHAPTER 2

[2.1] “Neurons, Neurotransmission and Communication”. In: The Nervous System. Capitolo 2. Academic Press, 2018, pp. 23-45.

[2.2] Min Suk Chung, Beom Sun Chung, “Morphology of the central nervous system”, Visually Memorable Neuroanatomy for Beginners - Chapter 1, Academic Press, 2020, Pages 1-43

[2.3] B.J. Richmond, “Information Coding”, Encyclopedia of Neuroscience, Academic Press, 2009, Pages 137-144

[2.4] Edmund T. Rolls, “The cingulate cortex and limbic systems for action, emotion, and memory”, Handbook of Clinical Neurology - Chapter 2, Elsevier, Volume 166, 2019, Pages 23-37

[2.5] Shnayder, Natalia A., Timur K. Sirbiladze, Irina V. Demko, Marina M. Petrova, and Regina F. Nasyrova. 2022. "Limbic Encephalitis Associated with COVID-19" Encyclopedia 2, no. 1: 26-35. https://doi.org/10.3390/encyclopedia2010003

[2.6] Al-kuraishy, Hayder & Raad, Nawar & Salih, Marwa & Al-Gareeb, Ali & Al-Mamoori, Farah & Albuhadilly, Ali. (2021). The Potential Role of Pancreatic γ-Aminobutyric Acid (GABA) in Diabetes Mellitus: A Critical Reappraisal. International Journal of Preventive Medicine. 12.

[2.7] Oscar Marin, John L.R. Rubenstein, “Patterning, Regionalization, and Cell Differentiation in the Forebrain”, Mouse Development, Academic Press, 2002, Pages 75-106;

[2.8] Bioimaging And Brain Research A.A. 2021/2022 teaching material, professor Camillo Porcaro (Università Politecnica delle Marche, now Università Politecnica di Pavia).

[2.9] Gurugirijha Rathnasamy, Wallace S. Foulds, Eng-Ang Ling, Charanjit Kaur, Retinal microglia – A key player in healthy and diseased retina, Progress in Neurobiology, Volume 173, 2019, Pages 18-40, ISSN 0301-0082, https://doi.org/10.1016/j.pneurobio.2018.05.006.

[2.10] Mecarelli, O. (2019). Clinical Electroencephalography. Page 11. https://doi.org/10.1007/978-3-030-04573-9

[2.11] Jay B. Angevine, Carl W. Cotman *From Principles of Neuroanatomy, by Jay B. Angevine, Jr., and Carl W. Cotman, copyright 1981 by Oxford University Press, Inc.*

CHAPTER 3

[3.1] Niedermeyer, E., Schomer, D. L., & H., L. da S. F. (2011). Chapter 1 to 6. In Niedermeyer's electroencephalography: Basic principles, clinical applications, and related fields. essay, Wolters Kluwer Health/Lippincott Williams & Wilkins.

[3.2] Drummond L. Pathological EEG phenomena and their significance. In: Alarcón G, Valentín A, eds. Introduction to Epilepsy. Cambridge University Press; 2012:96-106. Page 96.

[3.3] Biomedical Instrumentation_ Technology and Applications-McGraw-Hill Professional (2004). p. 170-178 Khandpur, Raghbir

[2.4] EEG signal processing-John Wiley & Sons (2007). p. 1-13 Sanei, Saeid e Chambers, J. A.

[3.4] Systematic comparison between a wireless EEG system with dry electrodes and a wired EEG system with wet electrodes. J.W.Y. Kam, S. Griffin, A. Shen, S. Patel, H. Hinrichs, H.J. Heinze, L.Y. Deouell, R.T. Knight. Neuroimage, 2019.

[3.5] Minmin Miao, Longxin Zheng, Baoguo Xu, Zhong Yang, Wenjun Hu, A multiple frequency bands parallel spatial–temporal 3D deep residual learning framework for EEG-based emotion recognition, Biomedical Signal Processing and Control, Volume 79, Part 2, 2023, 104141, ISSN 1746-8094, https://doi.org/10.1016/j.bspc.2022.104141.

[3.6] Zheng, Wei-Long (56377405900); Lu, Bao-Liang, Investigating Critical Frequency Bands and Channels for EEG-Based Emotion Recognition with Deep Neural Networks (2015) IEEE Transactions on Autonomous Mental Development, 7 (3), art. no. 7104132, pp. 162 - 175, Cited 1203 times. DOI: 10.1109/TAMD.2015.2431497

[3.7] Xia, X., Hu, L. (2019). EEG: Neural Basis and Measurement. In: Hu, L., Zhang, Z. (eds) EEG Signal Processing and Feature Extraction. Springer, Singapore. https://doi.org/10.1007/978-981-13-9113-2_2

[3.8] Clarke, A.R., Barry, R.J., Karamacoska, D. et al. The EEG Theta/Beta Ratio: A marker of Arousal or Cognitive Processing Capacity?. Appl Psychophysiol Biofeedback 44, 123–129 (2019). https://doi.org/10.1007/s10484-018-09428-6

[3.9] Galvão, F., Alarcão, S. M., & Fonseca, M. J. (Year). Predicting Exact Valence and Arousal Values from EEG. Journal Name, Volume (Issue), pages. https://doi.org/10.3390/s21103414

CHAPTER 4

[4.1] Kumar, A., Lin, CC., Kuo, SH. et al. Physiological Recordings of the Cerebellum in Movement Disorders. Cerebellum 22, 985–1001 (2023). https://doi.org/10.1007/s12311-022-01473-6

[4.2] Kristian H. Reveles Jensen, Olalla Urdanibia-Centelles, Vibeke H. Dam, Kristin Köhler-Forsberg, Vibe G. Frokjaer, Gitte M. Knudsen, Martin B. Jørgensen, Cheng T. Ip, EEG abnormalities are not associated with poor antidepressant treatment outcome - A NeuroPharm study, European Neuropsychopharmacology, Volume 79, 2024, Pages 59-65, ISSN 0924-977X, https://doi.org/10.1016/j.euroneuro.2023.11.004.

[4.3] Martina Kopčanová, Luke Tait, Thomas Donoghue, George Stothart, Laura Smith, Aimee Arely Flores-Sandoval, Paula Davila-Perez, Stephanie Buss, Mouhsin M. Shafi, Alvaro Pascual-Leone, Peter J. Fried, Christopher S.Y. Benwell, Resting-state EEG signatures of Alzheimer's disease are driven by periodic but not aperiodic changes, Neurobiology of Disease, Volume 190, 2024, 106380, ISSN 0969-9961, https://doi.org/10.1016/j.nbd.2023.106380.

[4.4] Shivam Tiwari, Deepak Arora, Vishal Nagar, Supervised approach based sleep disorder detection using non - Linear dynamic features (NLDF) of EEG, Measurement: Sensors, Volume 24, 2022, 100469, ISSN 2665-9174, https://doi.org/10.1016/j.measen.2022.100469.

[4.5] Chen, X., Lin, J., Jin, H., Huang, Y., & Liu, Z. (2021). The psychoacoustics annoyance research based on EEG rhythms for passengers in high-speed railway. Applied Acoustics, 171, 107575. https://doi.org/10.1016/j.apacoust.2020.107575

[4.6] Klimesch, W. (2012). Alpha-band oscillations, attention, and controlled access to stored information. Trends in Cognitive Sciences, 16(12), 606–617. https://doi.org/10.1016/j.tics.2012.10.007

[4.7] Li, Z.-G., Di, G.-Q., & Jia, L. (2014). Relationship between electroencephalogram variation and subjective annoyance under noise exposure. Applied Acoustics, 75, 37–42. https://doi.org/10.1016/j.apacoust.2013.06.011

[4.8] Klimesch, W. (1999). Eeg Alpha and theta oscillations reflect cognitive and memory performance: A review and analysis. Brain Research Reviews, 29(2–3), 169–195. https://doi.org/10.1016/s0165-0173(98)00056-3

[4.9] Snipes, S., Krugliakova, E., Meier, E., & Huber, R. (2022). The Theta Paradox: 4-8 Hz EEG Oscillations Reflect Both Local Sleep and Cognitive Control. https://doi.org/10.1101/2022.04.04.487061

[4.10] Başar, E., Başar-Eroglu, C., Karakaş, S., & Schürmann, M. (2001). Gamma, alpha, Delta, and Theta oscillations govern cognitive processes. International Journal of Psychophysiology, 39(2–3), 241–248. https://doi.org/10.1016/s0167-8760(00)00145-8

[4.11] Barry, R. J., Johnstone, S. J., & Clarke, A. R. (2003). A review of electrophysiology in attention-deficit/hyperactivity disorder: II. event-related potentials. Clinical Neurophysiology, 114(2), 184–198. https://doi.org/10.1016/s1388-2457(02)00363-2

[4.12] Klimesch, W. (2012). Alpha-band oscillations, attention, and controlled access to stored information. Trends in Cognitive Sciences, 16(12), 606–617. https://doi.org/10.1016/j.tics.2012.10.007

[4.13] Er, M. B., Çiğ, H., & Aydilek, İ. B. (2021). A new approach to recognition of human emotions using brain signals and music stimuli. Applied Acoustics, 175, 107840. https://doi.org/10.1016/j.apacoust.2020.107840

[4.14] Yi Wen, T., & Mohd Aris, S. A. (2020). Electroencephalogram (EEG) stress analysis on alpha/beta ratio and theta/beta ratio. Indonesian Journal of Electrical Engineering and Computer Science, 17(1), 175. https://doi.org/10.11591/ijeecs.v17.i1.pp175-182

[4.15] W. -L. Zheng, J. -Y. Zhu, Y. Peng and B. -L. Lu, "EEG-based emotion classification using deep belief networks," 2014 IEEE International Conference on Multimedia and Expo (ICME), Chengdu, China, 2014, pp. 1-6, doi: 10.1109/ICME.2014.6890166.

[4.16] Xieqi Chen, Jianhui Lin, Hang Jin, Yan Huang, Zechao Liu, The psychoacoustics annoyance research based on EEG rhythms for passengers in high-speed railway, Applied Acoustics, Volume 171, 2021, 107575, ISSN 0003-682X, https://doi.org/10.1016/j.apacoust.2020.107575.

CHAPTER 5

[5.1] Songsamoe, S., Saengwong-ngam, R., Koomhin, P., & Matan, N. (2019). Understanding consumer physiological and emotional responses to food products using electroencephalography (EEG). Trends in Food Science & Technology, 93, 167–173. https://doi.org/10.1016/j.tifs.2019.09.018

[5.2] Jones, H. E., Herning, R. I., Cadet, J. L., & Griffiths, R. R. (2000). Caffeine withdrawal increases cerebral blood flow velocity and alters quantitative electroencephalography (EEG) activity. Psychopharmacology, 147(4), 371–377. https://doi.org/10.1007/s002130050005

[5.3] Clutterbuck, J. (n.d.). Mind monitor. Mind Monitor. https://mind-monitor.com/#page-top

[5.4] Zhang, R. (2018). The Effect of Meditation on Concentration Level and Cognitive Performance. Global Journal of Health Science, 11(1), 134. https://doi.org/10.5539/gjhs.v11n1p134

[5.5] EEGLAB official website: https://eeglab.org/

[5.6] Delorme, A., & Makeig, S. (2004). EEGLAB: An open source toolbox for analysis of single-trial EEG dynamics including independent component analysis. Journal of Neuroscience Methods, 134(1), 9-21.

CHAPTER 6

[6.1] van Dijk, H., deBeus, R., Kerson, C. et al. Different Spectral Analysis Methods for the Theta/Beta Ratio Calculate Different Ratios But Do Not Distinguish ADHD from Controls. Appl Psychophysiol Biofeedback 45, 165–173 (2020). https://doi.org/10.1007/s10484-020-09471-2

[6.2] Wafaa Khazaal Shams, Abdul Wahab, Imad Fakhri, Affective Computing Model Using Source-temporal Domain, Procedia - Social and Behavioral Sciences, Volume 97, 2013, Pages 54-62, ISSN 1877-0428, https://doi.org/10.1016/j.sbspro.2013.10.204.

[6.3] B. Conway, D. Halliday, S. Farmer, U. Shahani, P. Maas, A. Weir, and J. Rosenberg, “Synchronization between motor cortex and spinal motoneuronal pool during the performance of a maintained motor task in man.,” The Journal of physiology, vol. 489, no. Pt 3, p. 917, 1995.

[6.4] R. D. Fields and B. Stevens-Graham, “New insights into neuron-glia communication,” Science, vol. 298, no. 5593, pp. 556–562, 2002.
[6.5] S. Salenius and R. Hari, “Synchronous cortical oscillatory activity during motor action,” Current opinion in neurobiology, vol. 13, no. 6, pp. 678– 684, 2003.
[6.6] Sheida Malekpour, John A. Gubner, William A. Sethares,
Measures of generalized magnitude-squared coherence: Differences and similarities, Journal of the Franklin Institute, Volume 355, Issue 5, 2018, Pages 2932-2950, ISSN 0016-0032, https://doi.org/10.1016/j.jfranklin.2018.01.014.

CHAPTER 7

[7.1] Gary W. Evans and Dana Johnson, Cornell University. Stress and Open-Office Noise, Journal of Applied Psychology 2000, Vol. 85, No. 5, 779-783.
[7.2] Carlestam, G., Karlsson, C., & Levi, L. (1973). Stress and disease in response to exposure to noise: a review. In W. Ward (Ed.), Proceedings of the second international congress on noise as a public health problem. Report 550/9-73-008 (pp. 479–486). Washington, DC: EPA.
[7.3] A. Rabat, J.J. Bouyer, O. George, M. Le Moal, W. Mayo, Chronic exposure of rats to noise: Relationship between long-term memory deficits and slow wave sleep disturbances, Behavioural Brain Research, Volume 171, Issue 2, 2006, Pages 303-312, ISSN 0166-4328.